A FEASIBILITY STUDY: METAL-ORGANIC FRAMEWORKS (MOFS) AS NOVEL DELIVERY SYSTEMS FOR ADSORPTION AND CONTROLLED RELEASE OF ALLYL ISOTHIOCYANATE (AITC)

By

ELHAM LASHKARI

A dissertation submitted to the

Graduate School-New Brunswick

Rutgers, The State University of New Jersey

In partial fulfillment of the requirements

For the degree of

Doctor of Philosophy

Graduate Program in Food Science

Written under the direction of

Professor Kit L. Yam

and approved by

_____

_____

_____

_____

New Brunswick, New Jersey

May, 2017

ABSTRACT OF THE DISSERTATION

A Feasibility Study: Metal-Organic Frameworks (MOFs) as Novel Delivery Systems for Adsorption and Controlled Release of Allyl Isothiocyanate (AITC)

By ELHAM LASHKARI

Dissertation Director:

Professor Kit L. Yam

This research investigated the technical feasibility of metal- organic frameworks (MOFs) as novel delivery systems for adsorption and controlled release of volatile allyl isothiocyanate (AITC) molecules. We hypothesized that water vapor molecules could act as an external stimulus to trigger the release of AITC molecules adsorbed in MOFs. To test this hypothesis, three MOFs—HKUST-1, MOF-74(Zn), and RPM6-Zn—were selected based on their structural properties and AITC molecular characteristics. Results from adsorption-desorption and GC headspace analyses showed that these MOFs could encapsulate and retain AITC molecules within their pores under low (30-35%) relative humidity (RH) conditions. In contrast, the release of AITC molecules from all these MOFs was triggered under high RH (95-100%) conditions. These findings along with results from SEM, TEM, and XRPD studies support our hypothesis that water vapors could trigger the AITC release from these MOFs, indicating that development of the AITC-MOFs delivering system is technically feasible.

Acknowledgment

The completion of my Ph.D. dissertation and research would not have been possible without the kind support and help of many individuals. I would like to extend my sincere thanks to all of them. Foremost, I want to offer this endeavor to God almighty for the wisdom and strength he bestowed upon me in order to finish this project.

I am grateful to all those with whom I have had pleasure to work with during my PhD studies. I would like to express my special thanks and gratitude to my advisor Prof. Kit L. Yam whose expertise, understanding, and generous guidance and support make it possible for me to work on this project. It was a pleasure to work with him.

I am greatly indebted to Prof. Jing Li for her precious expertise, kind advice, and being a source of motivation in this research. It was an honor working with her. I also want to thank my colleague Hao Wang for providing me with MOFs and his assistance and collaboration along the way in this project.

I would like to express my deep gratitude to my family for their encouragement and support that helped me in completion of my studies. Special thanks to my loving and supportive husband, Yasser, for always being on my side during the time I needed him most and helped me in the pursuit of my goals.

I would like to thank my committee member Dr. Liu and Mr. Uknalis from USDA-ARS-ERRC for their support and assistance in obtaining SEM and TEM images for this research work. Also I am thankful to Prof. Takhistov for serving as one of my committee members.

My thanks and appreciations also go to all friends, lab mates, classmates, and colleagues who support and help me on this project and other activities during my PhD studies.

Last but not least, I extend my deep gratitude to all faculties and staff members especially Bill, Dave, Debbie, and Yakov who offered me help and support during different stages of my studies.

Table of Contents

List of Tables

List of Figures

1. Introduction

A major challenge of the food industry is to reduce the conventional use of synthetic food preservatives and substitute them with their natural counterparts in food formulations. Natural preservatives are perceived to have lower toxicity, less negative environmental effects, and better consumer acceptance. For these reasons, the potential use of essential oils or their natural bioactive compounds as plant derived antimicrobial agents for preservation of various food products has received much interest recently (Tyagi and Malik, 2010; Laird and Philips, 2011; Hyldgaard et al., 2012). Allyl isothiocyanate (AITC), a potent natural antimicrobial compound (Frankel et al., 2016), is derived mostly from plants such as mustard seeds, horseradish, broccoli, and wasabi. It possesses outstanding antimicrobial characteristics against a broad spectrum of foodborne pathogens and food spoilage-inducing microorganisms especially in vapor phase even at low concentrations (Inouye et al., 1983; Goi et al., 1985; Isshiki et al., 1992; Delaquis and Sholberg, 1997). AITC is typically added directly as a food-flavoring agent to meats, mustard and mayonnaise condiments, but there is also a good opportunity to add AITC as a natural preservative to improve food safety.

However, the direct addition of AITC to food products has two major limitations. First, AITC is unstable when added directly to the food product, as it may react or bind to some food components such as water, peptides, and amino acids that eventually may result in degradation or unavailability of all or part of added AITC. Consequently, sufficient amounts of AITC no longer exist to act as an efficient natural food preservative (Chen and Ho, 1998; Nadarajah et al., 2005; Chacon et al., 2006). Second, its pungency when used at high concentrations is another limiting factor that hinders its direct

incorporation into food matrices. To overcome the limitations of direct addition, this study proposes the use of metal-organic frameworks (MOFs) as novel delivery or carrier systems for adsorption and controlled release of volatile AITC molecules. This novel antimicrobial packaging approach allows the successful implementation of AITC into food systems by improving its stability while eliminating or reducing its negative organoleptic impact on various food matrices (Plackett et al., 2007; Kim et al., 2008; Park et al., 2012; Dias et al., 2013; Siahaan et al., 2014; Kara et al., 2014; Otoni et al., 2016).

The uniqueness of this approach is that the volatile AITC molecules can penetrate more easily into the bulk of food matrices, and its carrier (the MOFs particles) does not need to be in direct contact with the food. Metal-Organic Frameworks (MOFs) are a novel class of highly ordered crystals with 3D network structures. They are formed through self-assembly of metal ions or clusters —mostly transition metals such as Cu, Zn, and Fe— that are connected together by organic ligands as linkers. These frameworks are highly porous and possess remarkable inner surface areas (Huang et al., 2003; Mueller et al., 2006). Their inner channels or pores even can be tailored based on the desired functionality and characteristics of the guest molecules. These features make MOFs suitable candidates as delivery systems for adsorption and controlled release of small vaporous bioactive compounds such as volatile AITC molecules. While MOFs has significant structural diversity and robust thermal and mechanical stability, their high affinity to water molecules can sometimes lead to structural breakdown (Rosi et al., 2005; Greathhouse and Allendorf, 2006; Küsgens et al., 2009; Toni et al., 2012; Vaughn et al., 2013). This behavior may be used as a tool to induce release of entrapped AITC molecules from selected MOFs.

In this research, we hypothesized that the high amounts of relative humidity within the package of high moisture content food products such as fresh produce can act as an external trigger for the release of entrapped AITC molecules from selected MOFs in a timely manner. To our knowledge this study would be the first attempt to investigate the technical feasibility of these frameworks as novel AITC carriers for food safety and food industry applications.

2. Technical Background

2.1 Allyl Isothiocyanate (AITC, $CH_2=CHCH_2N=C=S$)

Allyl isothiocyanate is a natural volatile bioactive compound mostly found in plants from Cruciferae family (shown in Figure 1) such as mustard seeds, horseradish, cabbage, broccoli, and Japanese wasabi (Lin et al., 2000; Kim et al., 2002; Li et al., 2007; Neoh et al., 2012). AITC is formed by the enzymatic hydrolysis of the Cruciferous plant tissue glucosinolates that are sulfur-containing products (e.g. sinigrin) by myrosinase, a cell wall-bound enzyme (Delaquis and Mazza, 1995).

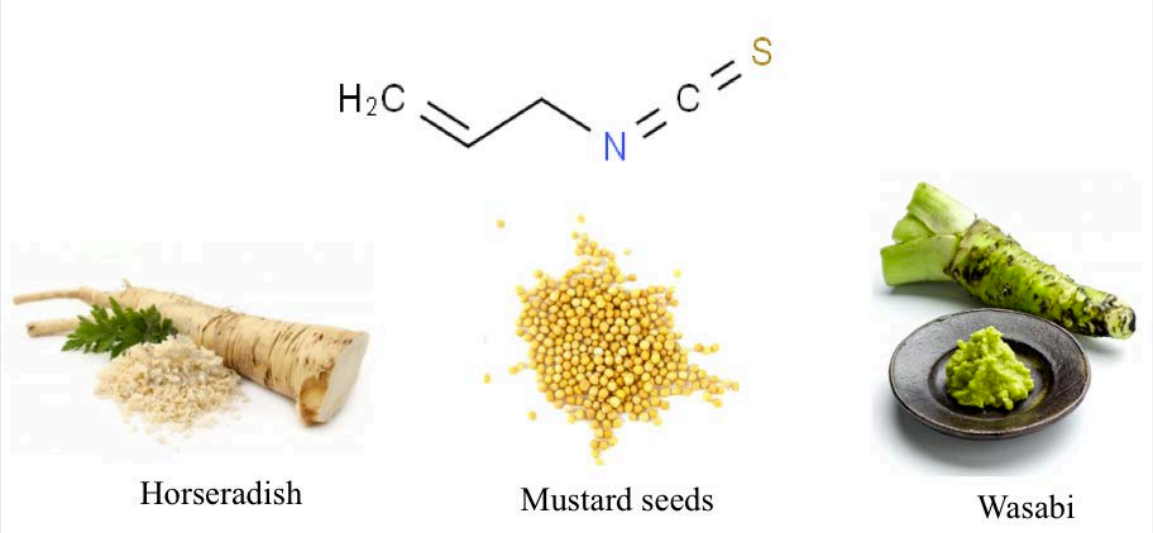

Figure 1. Chemical structure of allyl isothiocyanate (AITC) and some AITC containing plants.

Table 1 provides information on the natural occurrence of AITC in various plants. The AITC concentrations in some of these plants can vary considerably. For example, the AITC concentration in mustard seeds range from 400 to 15000 mg/kg depending on the species of the seeds. Shredded cabbage and coleslaw contain 3-17 mg/kg AITC (Delaquis and Mazza, 1995).

Table 1. Concentration of natural occurrence of AITC in plants

Plant	Concentration (mg/kg)
Mustard	400-15000
Horseradish	1500-9000
Wasabi	9585
Cabbage	0.04-3.0
Cauliflower	0.08
Brussels Sprouts	0.1

Adapted from Stofberg and Grundschober (1987).

Currently AITC is mainly used as a food-flavoring agent in the food industry due to its pungent flavor. AITC is the main component of the mustard essential oil and is mainly used as a flavor enhancer in meats, mustard and mayonnaise condiments. AITC also possesses strong antimicrobial activity especially in its vapor form at low concentrations (Inouye et al., 1983; Goi et al., 1985; Delanquis and Sholberg, 1997). Yet, its application a natural preservative in food systems is limited for the following reasons. AITC is highly volatile with poor water solubility and pungent flavor when used at moderate concentrations. Additionally, AITC reacts and binds to some food constituents such as amino acids and proteins or dissolve in fatty acids content of various food products that lead to its unavailability to act as an efficient food antimicrobial agent. It also decomposes in aqueous solutions that weaken its antimicrobial efficiency (Kawakishi and Namiki, 1969; Chen and Ho, 1998). In spite of these limiting factors, interests in using AITC as a natural food preservative is rising because of its natural origin and its registration as a Generally Recognizes As Safe (GRAS) food additive within United States (FDA Code of Federal Regulations, 1999).

2.1.1 AITC: Chemical and Physical Characteristics

AITC is a colorless or pale yellow liquid with a pungent aroma. It is an aliphatic organic compound with a molecular formula of C_4H_5NS and molecular weight of 99.1 gr/mol. Its chemical name is 1-propene-3-isothiocyanate according to IUPAC. However, it has various other chemical synonyms and trade names including 2-propenyl-isothiocynate, allyl ester, allyl mustard oil, allyspol, senofoel, and volatile oil of mustard. AITC is slightly soluble in water (2 gr/L at 20 °C; 1:160-300) and is very soluble in most organic solvents such as ethanol (1:0.5), benzene, and ethyl ether (Hayes, 2011). AITC has boiling point within the range of 148-154 °C and its specific gravity at 20 °C is 1.0126 gr/cc. When heated up to decomposition or in contact with acid, it emits fumes of oxides of sulfur or nitrogen and cyanides (Lewis, 2004). Odor threshold of 8×10^{-3} ppm is also reported for AITC (Furia and Bellanca, 1975).

2.1.2 AITC: Stability and Reactions in Food Systems

Water and aqueous solutions- AITC is a strong electrophilic reagent that reacts readily with nucleophilic agents in foods such as water, hydroxyl ion, alcohols, amines, amino acids, and sulfate groups. It is reported that in aqueous media AITC gradually decomposes to unpungent and/or garlic-like odor products (Kawakishi and Namiki, 1969; Chen and Ho, 1998). Wakishi and Namiki (1969) also proposed that the decomposition mechanism of AITC in aqueous media is a nucleophilic addition reaction on –N=C=S end rather than a hydrolysis reaction. According to these researchers, the nucleophilic addition reaction results in the formation of few other products that is shown in Figure 2.

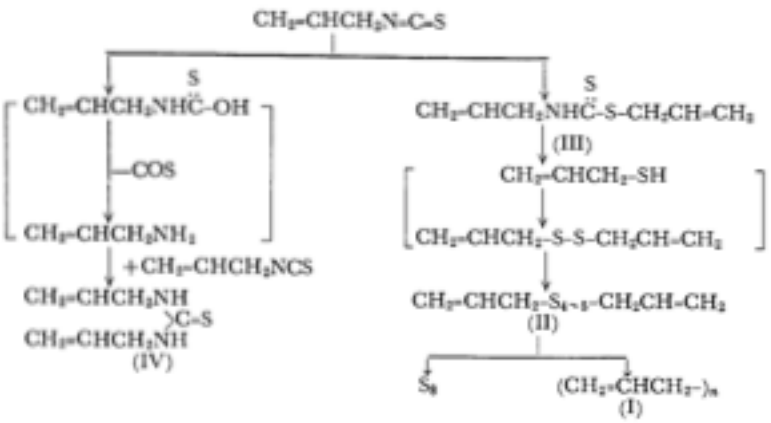

Figure 2. Proposed degradation diagram of AITC in aqueous media. II, III, IV, and I stand for the main decomposition products (Adapted from Kawakishi & Namiki, 1969).

It is demonstrated that both high temperature and alkaline condition accelerate decomposition of AITC in aqueous media (Ohta et al., 1995; Chen and Ho, 1998). Another study showed that the breakdown of AITC is slow under acidic condition even in aqueous phase of mayonnaise (Depree and Savage, 2001). Pecháček et al (1997) suggested pH 4 as the pH that AITC has the slowest decomposition rate in the solution medium. They also identified Allylamine, allyl dithiocarbamate, diallylthiourea, and carbon disulfide as the main reaction products of AITC in alkaline buffers.

Proteins, peptides, and amines- As mentioned earlier, AITC readily reacts with nucleophilic agents including amines and amino acids. AITC addition reactions with terminal amino group of peptides and amino acids such as argenine, lysine, and alanine in aqueous model systems result in the formation of *N*-allyl thiocarbamoyl peptide (ATC-peptide) and ATC-amino acid, respectively. 3-allyl-2-thiohydantoins is also the main derivative product of ATC-amino acid cyclization and/or cleavage of ATC-peptide under aqueous alkaline conditions (Kawakishi and Kaneko, 1987; Cejpek et al., 2000). Kawakishi and Kaneko (1987) also studied the interaction of AITC with thiol (R-SH) and

disulfide group of amino acids, proteins and peptides in model systems. Their results indicated that when cystine or cystine-containing peptides and proteins present in the experimental system, AITC induce oxidative cleavage of all or part of their disulfide bonds. In spite of multiple studies demonstrating reactions between AITC and peptide and proteins in model systems, whether AITC reacts with or binds to protein content of the food is not clear yet. A study conducted by Winther and Nielson (2006) on active packaging of cheese showed no sign of AITC decomposition or any of the reaction products between AITC and the cheese matrix, suggesting strong binding of AITC to the cheese matrix rather than its interaction with protein content of the cheese.

Fat and oil- AITC appears to be stable in oil for an extended period (Depree and Savage, 2001). AITC also is reported as a natural antioxidant agent, however the mechanism of its antioxidant effect in foods is not known well (Depree and Savage, 2001; Winther and Nielson, 2006).

It is worth mentioning that despite years of research, factors influencing AITC stability, secondary reactions, decomposition products and their mechanism of formations is still not fully understood.

2.1.3 AITC: Antimicrobial Characteristics

The antimicrobial effects of isothiocyanates (ITC) were known since the 10^{th} century in Japan, where it was widely believed that the chemical components in wasabi act as antimicrobials and are able to treat infections. Therefore, wasabi accompanied raw fish dishes such as sushi (Frankel et al., 2016). Application of AITC as a natural food preservative for food safety purposes has been studied since early 1930s (Isshiki et al., 1992). It has been well demonstrated that AITC has broad spectrum antimicrobial

properties both in culture media (Kojima et al., 1971; Isshiki et al., 1992; Park et al., 2012) and various food matrices; including ground and roasted beef (Ward et al., 1998; Nadarajah et al., 2005; Chacon et al., 2006), chicken breast (Shin et al., 2010), bakery products (Nielson and Rios, 2000), Cheese (Winther and Nielson, 2006), cooked rice (Kim et al., 2002), and fruits and vegetables (Mari et al., 2002; Seo et al., 2012; Piercey et al., 2012).

Mechanism of Action- The AITC's antifungal and antibacterial mode of action has not been fully understood, however, some mechanisms are suggested. In general, AITC is regarded as a non-specific inhibitor of periplasmic or interacellular targets since no single site of action is reported yet (Hyldgaard et al., 2012). According to Lin et al (2000), AITC damages the bacterial cell membrane causing the leakage of essential cellular metabolites. Thereby the antimicrobial mode of action of AITC is related to the general inactivation of essential intercellular enzymes and alternation of proteins through oxidative cleavage of their disulfide bonds (Delaquis and Mazza, 1995). Whether AITC rapidly crosses the membranes and enters the cytoplasm of prokaryotic and eukaryotic cells or its effects is on the cell membranes is not clear yet and demands further investigation. Various studies show that fungi are more sensitive to the effects of AITC than bacteria (Isshiki et al., 1992; Lin et al., 2000; Nielson and Rios, 2000). Nielson and Rios (2000) study showed that fungistatic and fungicidal effects of AITC depend on concentrations of both AITC and the spores. Moreover, it is reported that bactericidal and sporicidal effects of AITC varies with the type of bacterial starin, AITC concentration, temperature and time of exposure (Delaquis and Sholberg, 1997).

Table 2. Antimicrobial activity of Volatile AITC

Organisms	MID (µgr/dish)	MIC (ngr/mL)
"Bacteria"		
Bacillus subtilis IFO-13722	420	110
Bacillus cereus IFO-13494	360	90
Staphylococcus aureus IFO-12732	420	110
Staphylococcus epidermidis IFO-12993	420	110
Escherichia coli JCM-1649	110	34
Salmonella typhymurium ATCC-14028	210	54
Salmonella enteritidis JCM-1891	420	110
Vibrio parahaemolyticus IFO-12711	210	54
Pseudomonas aeruginosa IFO-13275	210	54
"Yeast"		
Saccharomyces cerevisiae NFRI-3066	62	22
Hansenula anomala NFRI-3717	124	37
Torulaspora delbreuckii NFRI-3811	50	18
Zygosaccharomyces rouxii NFRI-3447	31	16
Candida tropicalis NFRI-4040	62	22
Candida albicans IFO-1061	62	22
"Molds"		
Aspergillus niger ATCC-6275	124	37
Aspergillus flavus NFRI-1157	124	37
Penicillium islandicum NFRI-1156	62	22
Penicillium citrinum NFRI-1019	62	22
Penicillium chrysogenum IFO-6223	250	62
Fusarium oxysporum NFRI-1011	62	22
Fusarium graminearum NFRI-1233	31	16
Fusarium solani IFO-9425	110	34
Alternaria alternata IFO-4026	62	22
Mucor racemosus IFO-6745	250	62

- Growth of bacteria and yeast was observed for 2 days. Growth of molds was observed for 7 days. MID: minimum inhibitory dose; MIC: minimum inhibitory concentration in headspace gas (Isshiki et al., 1992)

AITC Vapor vs. liquid form- as demonstrated in Table 2, AITC is significantly more effective against spoilage bacteria and food-borne pathogens in its vapor phase at relatively lower concentration (Isshiki et al., 1992). Sekiyama et al. (1996) reported that AITC vapor is 500 to 1000 times more effective than the same amount of liquid AITC in agar medium. It is suggested that the higher efficacy might be due to better penetration

ability of active constituents of the essential oil vapors into the microorganism cell membrane and the food matrices or culture medium that absorbed the vapor (Trivedi and Hotchandani, 2004; Malik and Tyagi, 2010). One other potential reason for its higher potency in vapor phase could be the fact that essential oils and their major bioactive compounds such as AITC are lipophilic molecules that in liquid form and aqueous media form micelles which subsequently suppress their attachment to the microorganisms, whereas the vapor phase that allows better attachment (Inouye at al., 2003). Moreover, usage of gaseous AITC has this advantageous that it can penetrate to the bulk food matrix and the direct contact between the food packaging polymer and the food itself is not necessary. Moreover, unlike non-volatile antimicrobial agents, essential oil volatiles also have this advantage that can cover a large surface area with no need or requirement for direct contact with the food surfaces.

2.1.4 AITC: Application as a Natural Food Preservative

Given the potent antimicrobial characteristics of AITC, recently its potential application as a natural food preservative for preservation of a wide range of food products becomes the topic of interest among researchers.

Direct addition of AITC to Foods- adding AITC directly to the food products for food safety application in food industry is limited to few spicy food products due to multiple reasons. It is highly volatile and has pungent aroma with poor water solubility. AITC also binds to and reacts with various nucleophilic food components (e.g. water, amines, amino acids, alcohols, and sulfites), which may result in its decomposition. Therefore, its decomposition or binding to food components makes AITC inaccessible to

act as an effective antimicrobial agent which in return required further addition of AITC to achieve the desired antimicrobial concentrations. On the other hand, the extra addition of AITC negatively impacts sensory attributes of most food products. To address these obstacles couple of approaches are suggested and examined so far.

Controlled release of AITC- controlled release of bioactive compounds such as AITC can be obtained through application of active antimicrobial packaging (AM), in which the microbial agent is added to the packaging material. Later, food-packaging film/coating allow the controlled release of active component into the food or the headspace surrounding the food over a long period of time. Additionally, food-packaging films can be designed to release the bioactive compounds as a response to environmental or thermal stimuli including moisture or temperature fluctuations. Although direct addition of AITC to the food packaging material has several advantages such as increasing the stability of AITC and reducing its negative sensory impact on the food, this method still faces some limitations. First, liquid AITC absorbs to most food packaging polymer materials. Second, its compatibility with the food packaging material as well as available surface area is limited. Finally, AITC diffusivity from the food packaging material to the outside environment of the food package over time is another limiting factor. Food-packaging film/coating also show limited sensitivity to the environmental moisture or temperature fluctuations (Vega-Lugo & Kim, 2009). Sachets, multilayer films and coatings are some of the packaging materials that are developed to provide controlled release of the bioactive compounds (Appendini and Hotchkiss, 2002; Li et al., 2012; Passarinho et al., 2014). Incorporation of volatile compounds in packaging films or coatings has this advantage that either the film or coating can reduce the

diffusion rate of the bioactive compound from the packaging material to the food headspace, thereby maintaining the bioactive compounds in the headspace or the surfaces of food products for an extended period of time.

Encapsulation of AITC- encapsulation of AITC improves its stability by preventing unnecessary interactions between AITC and other food components such as water, amines, and proteins. A variety of encapsulating methods are developed to provide physical entrapment of AITC through utilizing cyclodextrins, seaweed, gums (e.g. Arabic and calcium alginate gel beads), micro- and nanoemulsions (Chacon at al., 2006; Li et al., 2007; Kim et al., 2008; Liu and Yang, 2010; Ko et al., 2012; Neoh et al., 2012; Piercey et al., 2012; Siahaan et al., 2014). While these encapsulating systems aim to increase the stability of AITC in various food systems, each face some shortcoming as well.

Table 3. Developed encapsulating systems for AITC

Encapsulating Systems	Limitations	Reference
Micro- & Nanoemulsions	Limited to narrow group of foods	Chacon et al., 2006. Liu & Yang., 2010
Cyclodextrines	Strong binding → weak release	Padukka et al., 2000
Carbon nanotubes	Incorporation in liquid form required direct contact with food	Dias et al., 2013
Mesoporous silica	No trigger for release	Park et al., 2012
Electrospun fibers	Availability of equipment for production of nanofibers	Vega-lugo et al., 2009 Aytak et al., 2014. Kara et al., 2015
Mustard seed matrix powder	AITC production amount and release depend on the hydrolysis reaction	Dai & Lim., 2014
Br*own Seaweed*	Evenly distribution in food systems	Siahaan et al., 2014

For example, relatively strong physical interaction between β-cyclodextrin and flavor molecules may be challenging with respect to providing effective control release of

the encapsulated AITC (Padukka et al., 2000). Evenly distribution of encapsulated AITC in powder form in carriers such as edible brown seaweed is also a hurdle in complex food systems (Siahaan et al., 2014). On the other hand, in case of micro and nano-emulsions, their application is limited to a narrow group of food products, since the bioactive compound should be incorporated directly into the food systems that have both lipophilic and hydrophilic components such as butters, dressings, sauces, and various beverages. Dias and others (2013) also studied application of carbon nanotubes (CNT)[1] to encapsulate AITC for packaging shredded, cooked chicken meet. Since AITC was incorporated in both packaging film and CNTs in its liquid form, direct contact of the packaging material with the food surface was mandatory. The AITC release from both film and the CNTs were only diffusion dependent due to concentration gradient.

Encapsulation and Controlled Release of AITC- given the limitations that face various encapsulation technologies, recently adsorption of AITC by macro- and nano-particles as carriers and later inclusion of these complexes into the food packaging materials to provide controlled release of AITC becomes a subject of ongoing researches. These micro- and nanostructures have these advantages that not only offer a large surface area for loading of the bioactive compounds, but also are engineered to provide release of the bioactive compound in a controlled manner based on specific external stimuli such as relative humidity or temperature changes. Moreover, stability and consequently efficacy of AITC at lower concentrations for food safety application can be significantly improved without compromising their antimicrobial activity.

[1] Carbon nanotubes (CNTs) are nanoparticles made of entanglement of hundreds of individual tubes that are adhere to each other. (CNTs) form pores that can possibly hold active substances in their hollow inner cavity.

As an example, electrospun fibers of soy protein isolates (SPI), polylactic acid (PLA), and poly vinyl alcohol (PVA) are studied to encapsulate AITC molecules by exploiting the moisture-sensitivity of these nanofibers to trigger the release of AITC from the fiber carriers (Vega-Lugo A., and Lim L., 2009; Aytac et al., 2014). Dai and Lim (2014) also used the mustard seed matrix powder (MSMP) as both the source of AITC and its carrier to control the release of AITC by using the moisture in the air as the release trigger. These researchers reported that the amounts of released AITC from these microparticles depend on the ambient moisture, temperature and the particle size and/or oil content of the mustard seed powder. Although mustard seed powder can act a natural carrier, yet both production and release of AITC require precise control of the hydrolysis reaction of sinigrin[2]. Likewise, the hydrolysis of sinigrin also results in production of several other products in addition to AITC, including allyl thiocyanate, ally cyanade, and 1-cyano-2,3-epithiopropane, depending on the pH conditions which might affect and limits its application for various food products. Park et al. (2011 and 2012) investigated potential application of mesoporous silicas MCM-41 and SBA-15 as carriers for controlled release of AITC for food safety purposes. Their results showed that the pore network could be a suitable delivery system, and the controlled release was obtained by diffusion of embedded molecules from the pores. Yet, the AITC release is passive and is dependent on the pore diameters rather than a specific external stimulus such as moisture or temperature changes to trigger the release.

[2] Sinigrin is a glucosinolate naturally present in mustard seeds and other plants from *Cruciferae* family. When tissues of these plants are disrupted, the cell-bound myrosinase enzyme gets released, causing the hydrolysis of the glucosinolate sinigrin.

The focus of this PhD dissertation is to investigate the technical feasibility of a new class of microporous structures called metal-organic frameworks (MOFs) as novel encapsulating systems and controlled release agents for volatile AITC molecules.

2.2 Metal-Organic Framework

2.2.1 What Are MOFs?

Metal-organic frameworks, abbreviated to MOFs, are a novel class of highly ordered porous crystalline materials or solids that have attracted tremendous attention within the past two decades (Mueller et al., 2006; Horcajada et al., 2012). They have been also termed as metal-organic polymers, organic-inorganic hybrids, or porous coordination networks (Keskin & Kizilel, 2010). Although in some literature both metal-organic frameworks and coordinatation polymers are used interchangeably, according to IUPAC terminology, metal-organic frameworks are a subset of coordination networks[3] in which themselves are a subset of coordination polymers (Batten et al., 2013). Based on this classification while a coordination polymer is a coordination compound with repeating coordination entities extending in 1, 2, or 3 dimensions, a metal organic framework (MOF) is a coordination network with organic ligands containing potential voids. The 3D framework of MOFs is formed through self-assembly of metal ions —mostly transition metals such as Cu, Zn, or Fe—, metal clusters, or metal-oxygen clusters acting as coordination centers that are linked together by various multitopic organic ligands as linkers (e. g. polycarboxylates) (Figure 3). Rowsell and Yaghi (2004) defined three

[3] A coordination network has been defined as a coordination compound extending through repeating coordination entities in 2 or 3 dimensions, or through repeating coordination entities, in 1 dimension, but with cross-links between two or more individual chains, loops, or spiro-links.

characteristics that are required to consider a solid as a MOF: strong bonding providing robustness, linking units, and geometrically well-defined structures that imply that these solids must be highly crystalline.

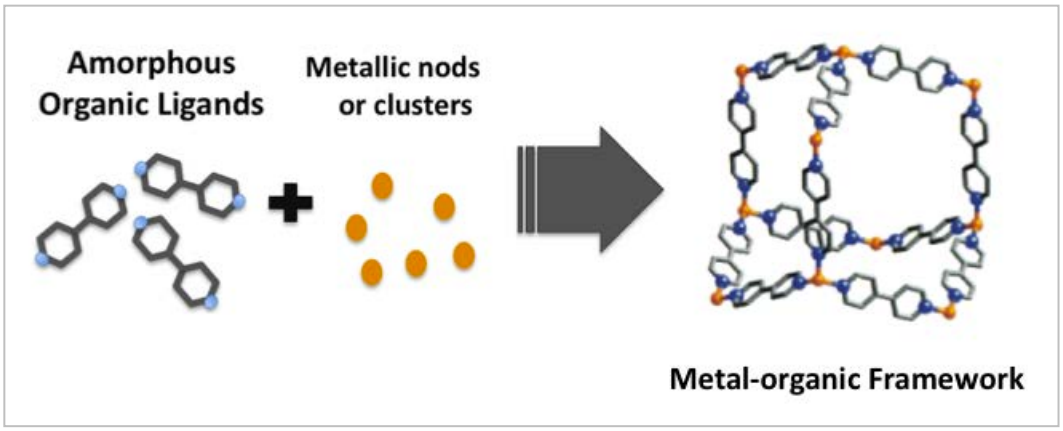

Figure 3. Structural components of MOFs (adapted from Eddaoudi et al. (2001) with some modification.

MOF Synthesis- in general MOFs are synthesized through solvothermal or hydrothermal techniques in which metal salts and organic ligands are combined and MOF crystals are slowly grown from a hot solution of metal precursors (below 300 °C). Water, dialkyl formamides, acetonitrile, and diethyl sulfoxide are some of the typical solvents used in these techniques. Later the MOFs are heated to remove the solvent that is used during the synthesis and remain inside the MOFs pores in a process called activation (Yaghi et al., 1995; Li et al., 1999; Yaghi et al., 2003; Kuppler et al., 2009). Temperature, concentration of metal salts and ligands, pH of the solution are some of the most important parameters during the solvothermal reactions. Other than the standard solvothermal method, MOFs can be synthesized by several other techniques including

electrochemical route, mixture of non-miscible solvents, and microwave irradiation (Kuppler et al., 2009).

2.2.2 Structural Properties of MOFs

The chemistry of MOF permits synthesis of an outstanding class of porous materials with highly porous structure and exceptional inner surface area (500-6000 m^2/gr) that far exceed the maximum surface areas of other existing porous structures such as zeolites, carbon nanotubes, mesoporous aluminosilica, aerogels, and activated carbon (Küsgens et al., 2009; Zaworotko, 2010). MOFs typically have low density (0.2-1 gr/cm^3) and reasonable thermal and mechanical stability. Given the large variety of inorganic building units and the large number of multitopic organic linkers, almost unlimited number of MOF structures can be synthesized. Variations in the organic linkers not only affect the pore size, but also generate materials with different chemical and functionalities and affinities for guest molecules.

The inorganic-organic hybrid in MOFs allow for more flexible design of the pore sizes (0.4-6 nm), shapes and surface functionality than their both inorganic (zeolites) and organic counterparts (Huang et al., 2003; Horcajada et al., 2012). However, MOFs networks can be either rigid or flexible. The rigid MOFs possess permanent porosity and robust frameworks similar to inorganic porous materials such as silica (Si-O). On the other hand, flexible ones possess dynamics and respond to external stimulus such as guest molecules, temperature and pressure. This flexibility of structure, also known as “breathing”, sometimes allows the pores to reversibly adjust to the size of the adsorbate. The structural flexibility in MOFs is attributed to the coordination bonds such as metal-

oxygen and metal-nitrogen that are less rigid than strong covalent bonds in porous materials such as silica allowing the MOF to shrink or expand when interact with the guest molecules. They also lack non-accessible bulk volume that offers one of the highest porosities (Mueller et al., 2006). The key advantage of MOFs over other well-known porous materials such as zeolites and carbon nanotubes is that their inner channels can be designed or modified during synthesis to host various guest molecules. Through selection of appropriate building blocks, thereby tenability allows synthesis of a wide range of architectures and functionalities (Keskin and Kizilel, 2010; McKinlay et al., 2010; Horcajada et al., 2012).

2.2.3 Applications of MOFs

The enormous number of distinct MOFs provides a great opportunity to implement them for various applications in different fields. The unique features of MOFs including high porosity, significant surface area, lack of non-accessible voids, wide range of pore sizes and shapes make them suitable candidates for various applications in chemical engineering, chemistry, material science, and biomedical fields. MOFs are classified as microporous materials with pore size less than 20 Å. The small pore sizes cause strong interaction between the small gaseous molecules as guests and the walls of the pores, makes these structures well-suited for gas adsorption, storage and separation applications (Eddaoudi et al., 2000; Lee et al., 2005; Pan et al., 2006; Frost et al., 2006; Li and Yang, 2007; Lan et al., 2009, Zhang et al., 2010; Xu et al., 2013). MOFs with flexible structures also considered promising for application in molecular sieving and sensing. Applications of MOFs in medicine for drug storage and delivery, luminescence and sensor technology, shape and size-selective catalysis, molecular magnetism, and heat transformation for

cooling applications have become a field of endeavor for researchers as well (Pan et al., 2006; Kuppler et al., 2009; McKinlay et al., 2010; Janiak and Vieth, 2010, Wu et al., 2012).

MOFs as Novel Carriers of Bioactive Compounds- MOFs have high loading capacity due to their high porosity and are biodegradable, at least to some degree. They can also be detected through imaging techniques and are also able to control the release of the encapsulated compound by avoiding the "burst effect[4]" (Horcajada et al., 2010). These interesting features make MOFs suitable as delivery vectors and controlled release agents of drugs and bioactive compounds, thereby their applications for biological and medicinal purposes have received tremendous attention recently (An et al., 2009; McKinlay et al., 2010; Horcajada et al., 2010; Horcajada et al., 2012). MOFs applications as nano-encapsulating agent for drug delivery (Horcajada et al., 2010; McKinlay et al., 2010) and as a carrier for controlled release of small fragrant molecules (RPM series) (Vaughn et al., 2013) suggest that their potential application as delivery systems to adsorb and later release volatile AITC antimicrobial molecules in a controlled manner for food safety purposes may be feasible.

For medicinal application both functionality and biocompatibility of MOFs must be taken into consideration. For this reason, constructing bio-MOFs or MOFs that are build from simple biomolecules and biocompatible metal cations currently become another field of study for researchers (An et al., 2009; Horcajada et al., 2010; Horcajada et al., 2012). However, MOFs applications as carriers of volatile antimicrobial agents for

[4] Burst effect: significant release (e.g. drugs) within the first minutes.

food safety purposes do not necessarily required either direct addition or even contact with the food products. One strategy is to incorporate MOF-antimicrobial complexes into the antimicrobial-releasing sachets and place them within the enclosed food packaging material. The sachets materials are required to be permeable to the antimicrobial agent.

3. Hypothesis and Objectives

To overcome the limitations of direct addition of AITC to food products, this study proposes the use of metal-organic frameworks (MOFs) as novel delivery or carrier systems for adsorption and controlled release of volatile AITC molecules. This novel antimicrobial packaging approach allows the successful implementation of AITC into food systems by improving its stability while eliminating or reducing its negative organoleptic impact on various food matrices (Plackett et al., 2007; Kim et al., 2008; Park et al., 2012; Dias et al., 2013; Siahaan et al., 2014; Kara et al., 2014; Otoni et al., 2016). The uniqueness of this approach is that the volatile AITC molecules can penetrate more easily into the bulk of food matrices, and its carrier (the MOFs particles) does not need to be in direct contact with the food. These frameworks are highly porous and possess remarkable inner surface areas (Huang et al., 2003; Mueller, Schubert, Teich, Puetter, Schierle-Arndt, and Pastre, 2006). These features make MOFs suitable candidates as delivery systems for adsorption and controlled release of small vaporous bioactive compounds such as volatile AITC molecules. While MOFs has significant structural diversity and robust thermal and mechanical stability, their high affinity to water molecules can sometimes lead to structural breakdown (Rosi et al., 2005; Küsgens et al., 2009; Vaughn et al., 2013). This behavior may be used as a tool to induce release of entrapped AITC molecules from selected MOFs.

In this research, we hypothesized that the high amounts of relative humidity within the package of high moisture content food products such as fresh produce can act as an external trigger for the release of entrapped AITC molecules from selected MOFs in a timely manner (Figure 4). To our knowledge this study would be the first attempt to

investigate the technical feasibility of these frameworks as novel AITC carriers for food safety and food industry applications.

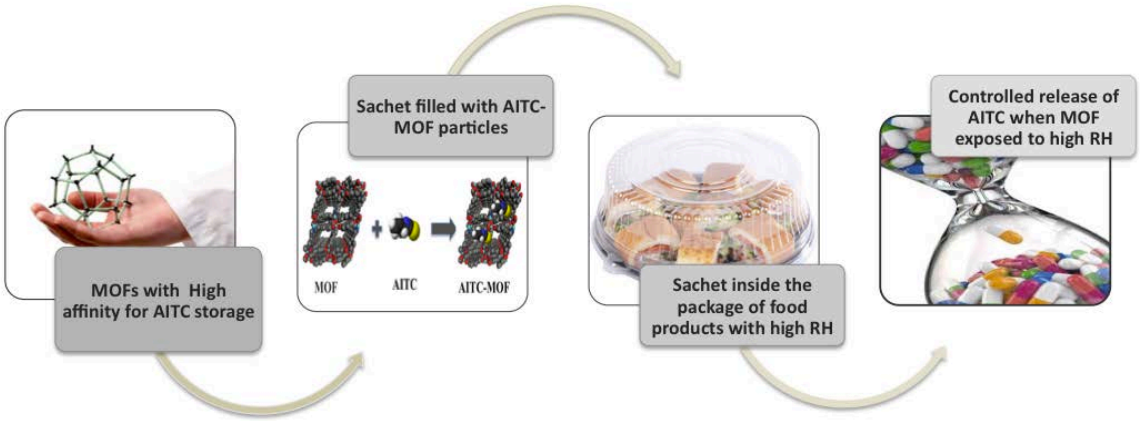

Figure 4. Schematic diagram of developing AITC-MOF delivery system for food safety applications.

To test this hypothesis, the main objectives of this study are as follows:

- To select and characterize MOFs able to efficiently adsorb and retain AITC vaporous molecules within their pores until their slow release being triggered by moisture.
- To investigate AITC loading capacity by the selected MOFs and the MOFs adsorption characteristics.
- To obtain controlled release profile of adsorbed AITC molecules in a timely manner in response to various environmental relative humidifies (% RH) and temperatures.
- To explore the underlying mechanism of AITC release from these selected MOFs.

4. Methods & Materials

4.1 Materials

AITC (>98% purity) was purchased from Matrix Scientific (Colombia, SC, USA). HKUST-1 microparticles were purchased from Sigma-Aldrich (St. Louis, MO, USA). MOF-74(Zn) and RPM6-Zn $[Zn_3(bpdc)_3(apy)]\cdot 3.08DMF$ (bpdc = biphenyl-4,4'-dicarboxylate, apy = 4,4'-azobispyridine) microparticles were synthesized and obtained from the Department of Chemistry and Chemical Biology, Rutgers University (Piscataway, NJ 08854). The preparation methods of the two MOFs is as follows:

Synthesis of RPM6-Zn- RPM6-Zn was prepared from $Zn(NO_3)_2\bullet 6H_2O$ (98%, Acros, 0.1485g, 0.5mmol) and ligands solutions 4,4'-apy (0.0460g, 0.25mmol) and biphenyl dicarboxylic acid (bpdc, Aldrich, 99%+, 0.1210g, 0.5mmol) in 10 mL DMF in a 20 mL glass vial by solvothermal technique. The mixture was homogenized for 2 min in an ultrasonic bath to agitate particles in the solution. Then the vial was heated in an oven at 100 ^oC for 20 hours and then cooled down naturally to room temperature. The reddish crystals were filtered and washed with DMF and dried in air. The complete crystalline data form single crystalline X-Ray diffraction study for RPM6-Zn can be found in Wang et al., (2016).

$$Zn(NO_3)_2\bullet 6H_2O + H_2bpdc + apy \xrightarrow[100\ ^oC]{DMF} Zn_3(bpdc)_3(apy)\bullet 6DMF$$

RPM6-Zn

***Synthesis of MOF-74(Zn)*:** the MOF-74(Zn) microparticles were prepared according to the methods published by Rowsell and Yaghi (2006). A mixture of zinc

nitrate hexahydrate (0.24 g, 0.8 mmol), 2, 5-dihydroxyterephthalic (0.08 g, 0.4 mmol), 9 ml DMF and 1 ml H_2O were transferred into a 28 ml Teflon-lined autoclave. The autoclave was then sealed and heated to 120 ˚C for 3 days. After filtering and washing with 20 ml DMF, the product was collected. Then the product was exchanged with 20 ml methanol in a glass vial every 2 h during daytime for at least 3 days. The solvent was removed under vacuum at 270 °C, yielding the porous material.

Pore characterization data and structural building components (types of metal and organic ligand) of the three MOFs are summarized in Table 4.

Table 4. Summary of selected MOFs pore characteristics and structural components

	HKUST-1	MOF-74(Zn)	RPM6-Zn
Organic linker(s)	1,3,5-benzene tricarboxylic acid	2,5-dihydroxyterephthalate	Linking ligand: biphenyl-4,4'-dicarboxylate Pillar ligand: 4,4'-azobispyridine
Metal	Copper	Zinc	Zinc
Pore size (Å)	Large pore: 9 Small pore: 6	5.5 × 10	7× 20
BET surface Area (m^2/gr)	1500-2100	496	609
Pore Volume (cc/gr)	0.71	NA	0.29
References	Küsgens et al., 2009 Moellmer et al., 2011	Britt et al., 2009 Glover et al., 2011	Wang et al., 2016

4.2 Methods

4.2.1 Adsorption and Quantification of Adsorbed AITC

Adsorption-desorption study was conducted to assess the affinities and loading capacities of these selected MOFs as encapsulating agents for volatile AITC molecules. During the adsorption phase, nitrogen was used as the carrier gas for AITC molecules by flowing through a liquid AITC bubbler at 18°C and bringing AITC vapor into the cavities of these microparticles. Following adsorption was the desorption phase in which pure nitrogen was flowing through the sample at 30°C so that AITC molecules loosely bound or adsorbed on the MOF surface rather than the inner cavities were washed away until a constant weight obtained. Sample weights were monitored and recorded during both phases of the experiment using a TA Instrument Q50 thermogravimetric analyzer (TGA).

4.2.2 GC Operating Condition

Headspace analysis of AITC was conducted using a 5890A Hewlett Packed gas chromatograph equipped with a DB-1 capillary column (30 m long, 0.32 mm inner diameter, 1 μm film thickness) and a flame ionization detector. The inlet and flame ionization detector temperatures were set at 220 and 250°C, respectively. Column temperature started at 50°C, held for 3 minutes, and then ramped from 50 to 180°C at a rate of 10°C/min. Helium was used as the carrier gas. The area under the curve for each concentration was obtained from the chromatograph software. Seven concentrations 2, 4, 10, 20, 40, 64, 100 ppm (as μL AITC/L air) of AITC (98% purity) were used to prepare the standard calibration curve (Figure 5). Each concentration was measured in triplicate.

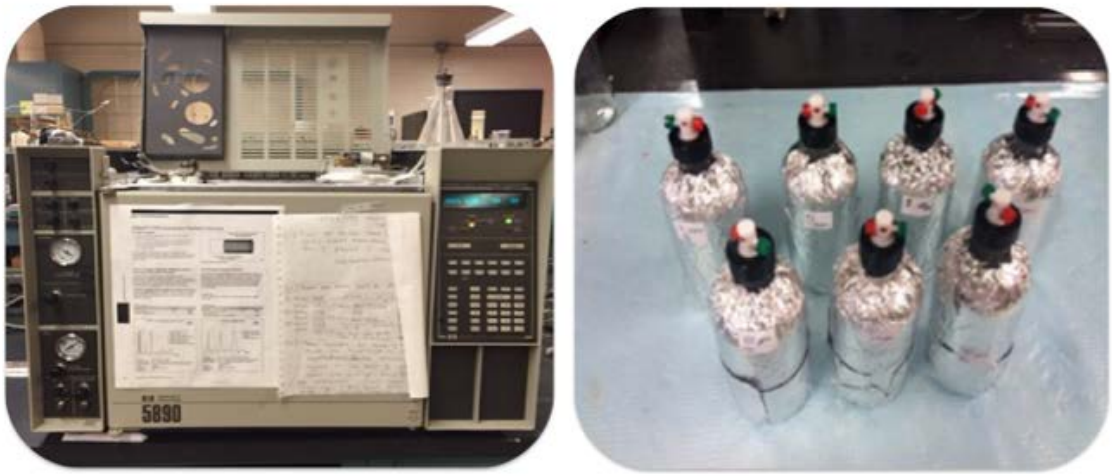

Figure 5. (Left) 5890A Hewlett Packed gas chromatograph; (right) 250 mL glass jars sealed with airtight valves for AITC headspace analysis.

4.2.3 AITC Release Measurements

Release kinetics of encapsulated AITC from the MOF microporous particles was studied by conducting GC headspace analysis under both high (95< %RH <100) and low (30< %RH <35) relative humidity conditions at room temperature (24±1°C). To produce and maintain high RH in 250 mL glass jars, 30 μL water was injected to each glass jar using a clean gas tight 0.5 mL syringe (Baton, Rouge, LA, USA) through the airtight valve (Mininnert valves, Supelco, Bellefonte, PA, USA) at the onset of the experiment. For low RH no water was added. 0.5 mL headspace samples were taken at predetermined time intervals to measure AITC concentration changes inside the jars. Pure liquid AITC (non-encapsulated AITC) was added to a filter paper in 250 mL glass jar as the control. All experiments were conducted with at least two repetitions. The effects of various temperatures on release profile of volatile AITC molecules from RPM6-Zn microparticles was studied under high RH at 6, 24, and 35 °C. As shown in Figure 6 the

temperature and relative humidity were monitored throughout the experiments by using mini digital thermometer and hygrometer temperature humidity gauges (amazon.com).

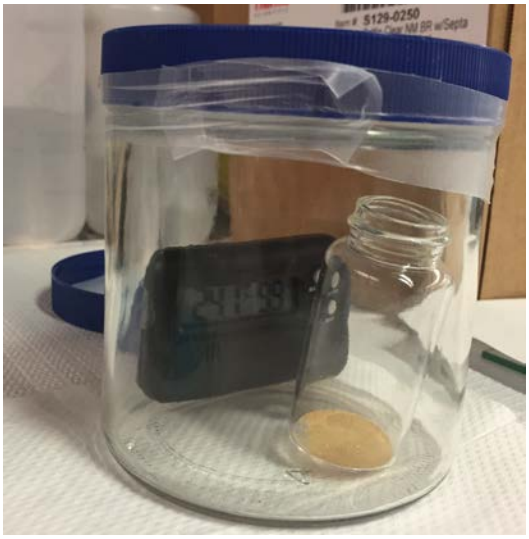

Figure 6. Monitoring the temperature and relative humidity (%RH) by using the mini-digital thermometer and hygrometer temperature humidity gauge.

4.2.4 Morphological Study of MOFs

To investigate the effects of moisture on structural characteristics of these microporous particles, SEM and TEM studies were conducted on MOF microparticles exposed to both low and high RH.

For SEM study, samples were mounted on stubs and sputter gold-coated by EMS 150R ES Sputter Coater (EM Sciences, Hatfield, PA) for 30 seconds (Figure 7, left). They were then observed under scanning electron microscopy, FEI Quanta 200F (Hillsboro, OR, USA) under an accelerating voltage of 5-10 KV in high vacuum mode.

For TEM, Formvar resin (EM Science, Hatfield, PA) was coated on a microscope slide and floated onto a water bath. Acetone clean cupper grids (200 mesh) placed on the film and then it was collected using a parafilm. A small amount of powders was pressed onto the grids. The grids then were observed under a Philips transmission microscope (CM-12, Philips, Netherlands) with an accelerating voltage of 80kV and imaged by using a DVC detector controlled by AMT software (Danvers, MA, USA).

4.2.5 X-ray Powder Diffraction Analysis (XRPD)

Powder X-ray diffraction analysis was performed on MOF samples before and after their exposure to low and high RH conditions to better understand the mechanism of AITC release from each MOF and the effect of moisture on AITC release from each MOF. MOF microparticles were finely distributed on a glassy lamella, and a Rigaku Ultima-IV X-ray diffractometer using Cu Kα radiation (λ = 1.5406 Å) was used to record the diffracted patterns of each sample (Figure 7, right). Graphite monochromator was used and the generator power settings were at 40 kV and 40 mA. Data were collected between a 2θ of 3–50° with a step size of 0.02° at a scanning speed of 2.0 deg/min.

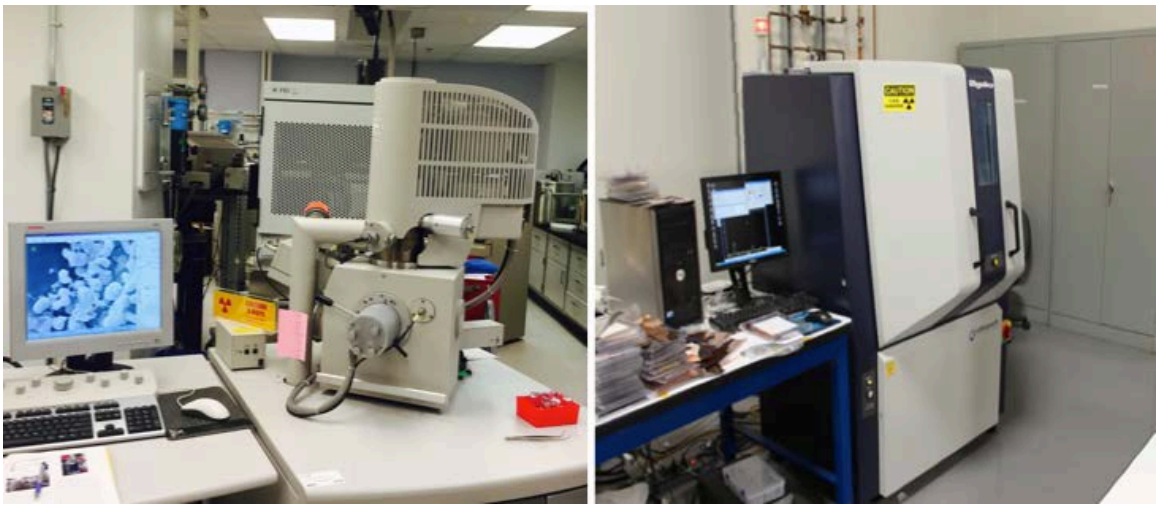

Figure 7. (Left) Scanning electron microscope (SEM); (right) Rigaku Ultima-IV X-ray diffractometer.

5. Results and Discussion

5.1 MOF Selection and Characterization

MOF selection for adsorption and controlled release of AITC molecules was based on two main factors: MOFs' pore size and their affinity or structural vulnerability to moisture.

MOFs' Pore Size- an efficient adsorption requires the encapsulating agent to be able to efficiently entrap and store the adsorbate molecules within its pores; as larger pores will lead to immediate release of the guest molecules, while pore sizes smaller than the size of the guest molecules will not allow absorption to occur. Therefore, as shown in Figure 8, the molecular dimension of AITC molecule (≈7.2 × 3.3Å) was taken into consideration for MOF selection.

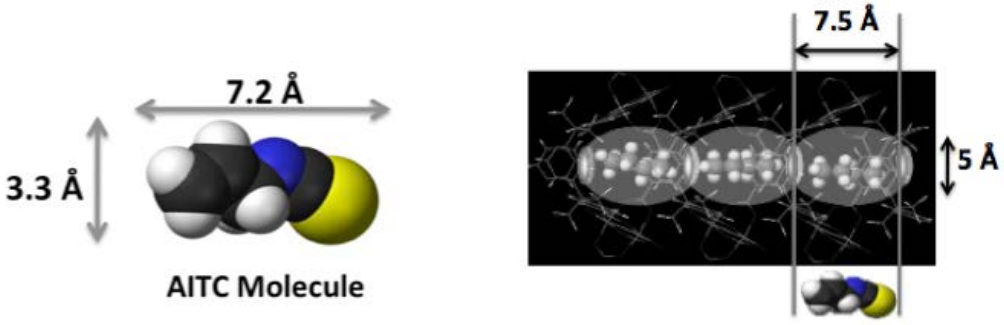

Figure 8. (Left) AITC molecular dimension; (right) illustration of AITC and MOF pore size matching for efficient adsorption of AITC molecules.

MOFs' structural vulnerability or affinity to moisture- MOFs affinity or structural vulnerability (Figure 9) can allow the moisture to act as the external stimulus to trigger

the release of encapsulated AITC molecules in a timely manner when the relative humidity in the headspace is high.

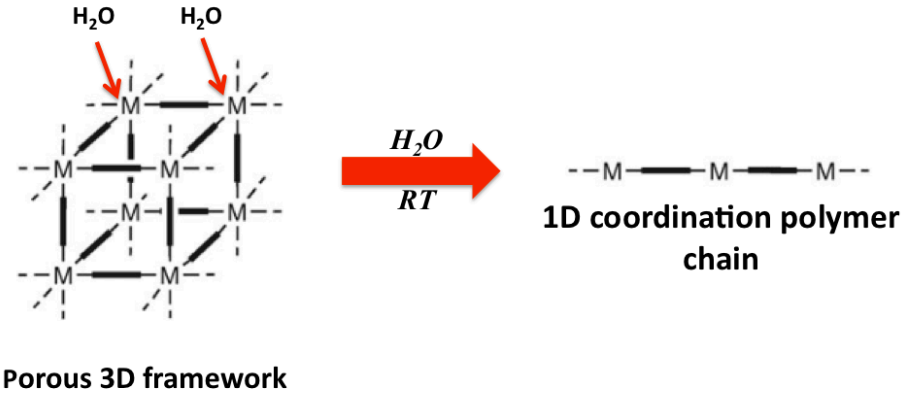

Figure 9. 3D structural breakdown of some MOFs by water molecules (the letter "M" represent metal nodes).

Given the above two main criteria, we selected three MOFs, HKUST-1, MOF-74(Zn), and RPM6-Zn,s as AITC encapsulating and delivery agents based on their structural properties including pore size and their affinity or sensitivity to water molecule. The summary of the MOFs pore characteristics and structural components is provided in Table 4. Further information on the chemical and structural properties of these MOFs is follows:

HKUST-1 *(Basolite™ C300):* is one of the most investigated MOFs in the literature due to its interesting properties especially in gas separation, storage, and catalysis fields (Küsgen et al., 2009; Lin and Hsieh, 2015). HKUST-1 or [Cu_3 $(BTC)_2$ $(H_2O)_3$] synthesis was first reported by researchers from “Hong Kong University of Science and Technology” (Williams et al., 1999). It is also among the first few MOFs that become commercially available due to its ease of synthesis and availability of its reagents. HKUST-1 possesses high inner surface area, accessible coordinatively

unsaturated metal sites (CUS) and high chemical stability (Lin et al., 2014; Lin and Hsieh, 2015). It is a cupper base MOF with bright blue crystals, and its microporous frameworks are made of cupper as the coordination centers that are connected through 1,3,5, benzene tricarboxylic acid as organic linkers (Figure 10).

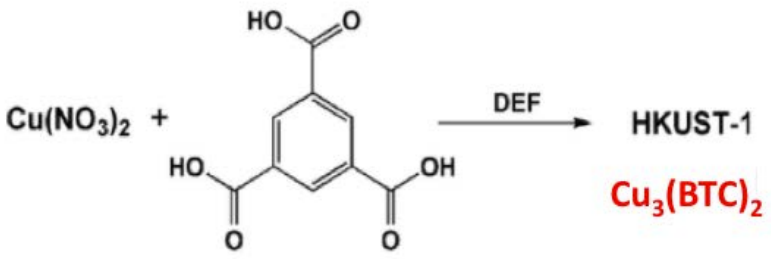

Figure 10. Main structural components of HKUST-1.

HKUST-1 exhibits a bimodal pore size distribution. As shown in the figure 11, the larger and more hydrophilic pores have a 9Å diameter. They consist of Cu_2(OOC–) paddle-wheel secondary building units (SBU) that each carries two metal coordination sites. The smaller pores are surrounded by 4 benzene rings with 6Å diameter, which make the pores interiors less hydrophilic.

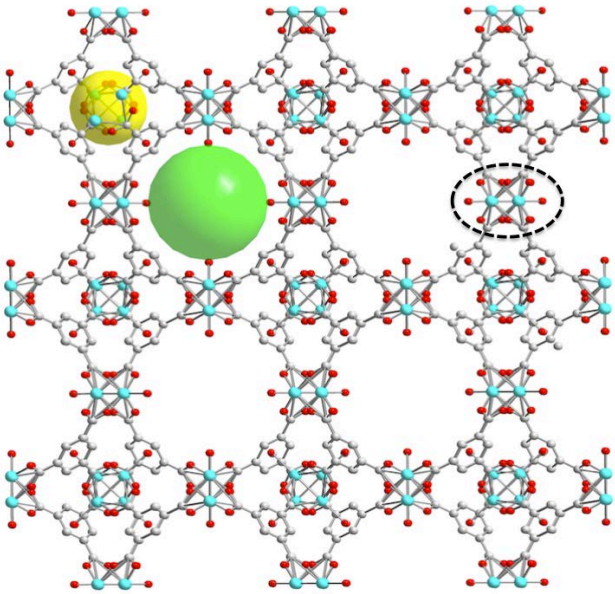

Figure 11. Chemical structural illustration of HKUST-1 in a two-dimensional view (teal:Cu, red:O, gray:C) with Cu-paddlewheel SBU in black dashed circle and large and small pores in green and yellow spheres.

MOF-74(Zn): also known as CPO-27-Zn is a Zn base MOF that metal sites are coordinated by carboxyl and hydroxyl groups of 2,5-dihydroxyterephtalate as the organic linker (Figure 12).

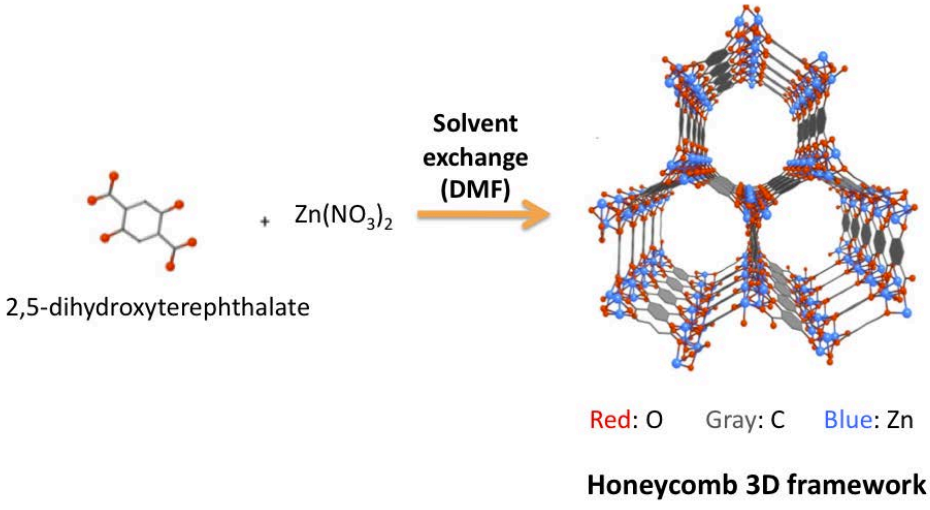

Figure 12. Main structural components of MOF-74(Zn) adapted from Britt et al., 2009 with modifications.

As shown in Figure 13, helical Zn-O-C rods are constructed from 6- coordinated Zn (II) centers, where each Zn has three carboxyl groups. The 1D inorganic rods are then linked by benzene units of organic linkers to form linear one-dimensional honeycomb (hexagonal) channels of 10.3 × 5.5 Å dimensions.

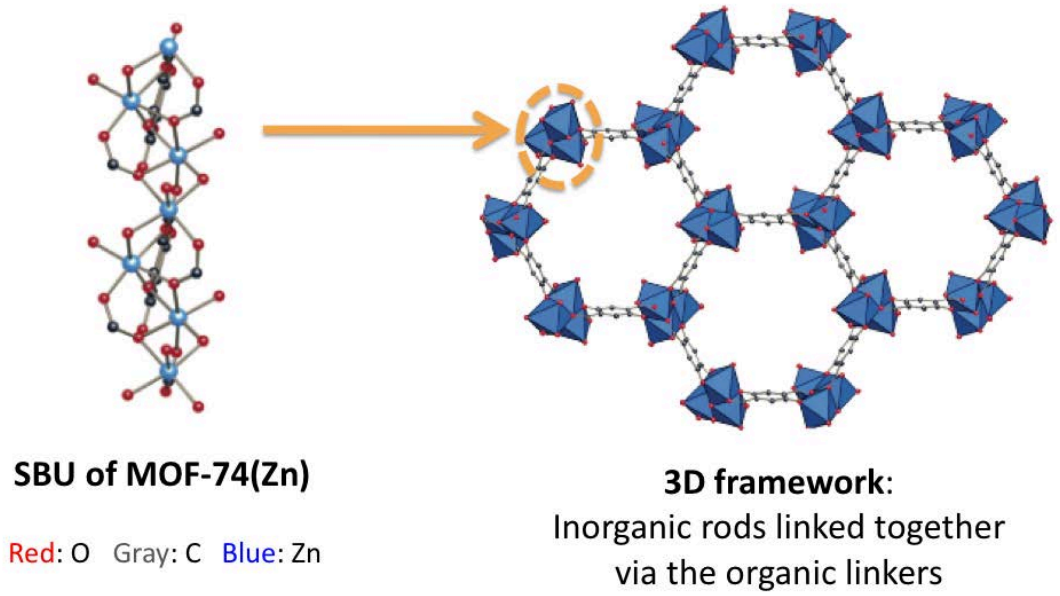

Figure 13. (Left) ball and stick representation of MOF-74(Zn); (right) the honeycomb 1D open channel of MOF-74(Zn) framework; inorganic SBUs linked together via benzene rings of organic ligands (gray) adapted from Rosi et al. (2005) with some modification.

RPM6-Zn *(Rutgers Recyclable Porous Materials):* the microporous framework of RPM6-Zn $[Zn_3(bpdc)_3(apy)]$•3.08DMF particles are composed of zinc metals as nods that are connected through biphenyl-4,4'-dicarboxylate (bpdc) as "linking ligands" and 4,4'-azobispyridine (apy) as "pillar ligands".

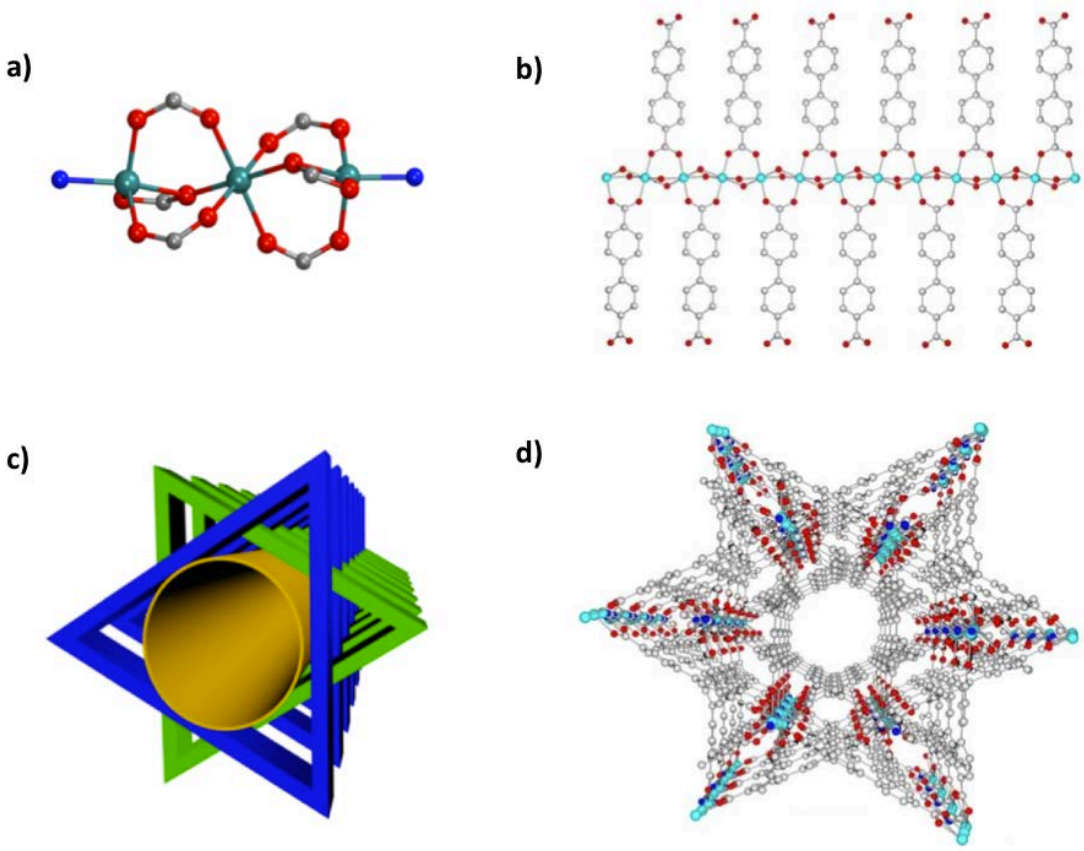

Figure 14. (a) SBU $Zn3(\mu2\text{-}OCO)_2(COO)_4$ of RPM6-Zn, (b) Zn(bpdc) 2D layer structure of RPM6-Zn, (c) two-fold interpenetrated nets to form 3D framework of RMP6-Zn, (d) 1D hexagonal channel of RMP6-Zn crystals (Zn: aqua, O:red, N:blue, C:gray) adapted from Wang et al. (2016) with some modifications.

The single crystal X-ray structure analysis is shown that RPM6-Zn possesses microporous 3D network, and two crystallographically independent zinc centers exist in RPM6-Zn 3D framework. One Zn center has formed six Zn-O coordinated bonds with carboxylate groups of bpdc linking ligands, while the other has formed five coordinated bonds with both linking and pillar ligands, 4 Zn-O coordination bonds with bpdc linking ligands and one Zn-N coordination bond with the pillar ligand. As shown in Figure 14a, the trinuclear secondary building unit (SBU), $Zn_3(\mu2\text{-}OCO)_2(COO)_4N_2$, is made of three

zinc centers and six carboxylate groups[5]. Each SBU is connected to six adjacent SBUs resulting in a two-dimentional (2D) layer parallel to bc plane (Figure 14b). The 2D layers are linked through 4,4'-azobispyridine (apy) "pillar ligand" to generate a 3D framework. Two of these 3D networks that are identical in structure, interpenetrate to yield a 3D porous framework of RPM6-Zn, with 1D open channels (window size: 7 Å × 20 Å) running along a direction with a hexagon-shaped cross-section (Figures 14c, d).

5.2 Adsorption and Quantification of Adsorbed AITC

The adsorption-desorption study was conducted to evaluate the potential application of these MOFs as carriers for adsorption and storage of AITC molecules. The adsorption-desorption profiles of AITC from these MOFs are shown in Figures 15, 16, and 17. The adsorption phase shows the loading or the mass of AITC adsorbed by the MOFs, while the desorption phase shows the mass of AITC retained by the MOF after nitrogen flushing. The small decline in mass during the desorption phase is due to the loss of some loosely adsorbed AITC molecules that were washed away by nitrogen. As shown in Figures 15, 16, and 17 the loading capacities are 42, 27, and 14% (mg AITC/gr MOF) for HKUST-1, RPM6-Zn, and MOF-74(Zn), respectively.

[5] Bridging ligand is preceded by the Greek character μ, and refers to a ligand that connects two or more atoms, usually metal ions. In this context, here μ2 stands for a bridging ligand that connects two metal ions.

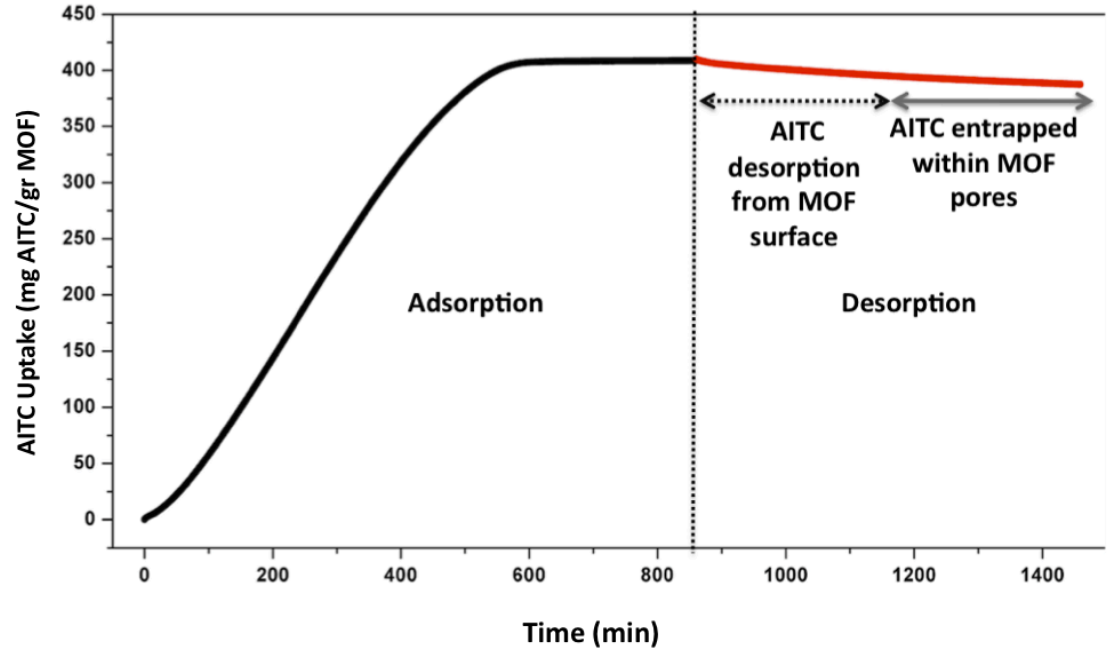

Figure 15. Adsorption-desorption profile of AITC on HKUST-1 microparticles.

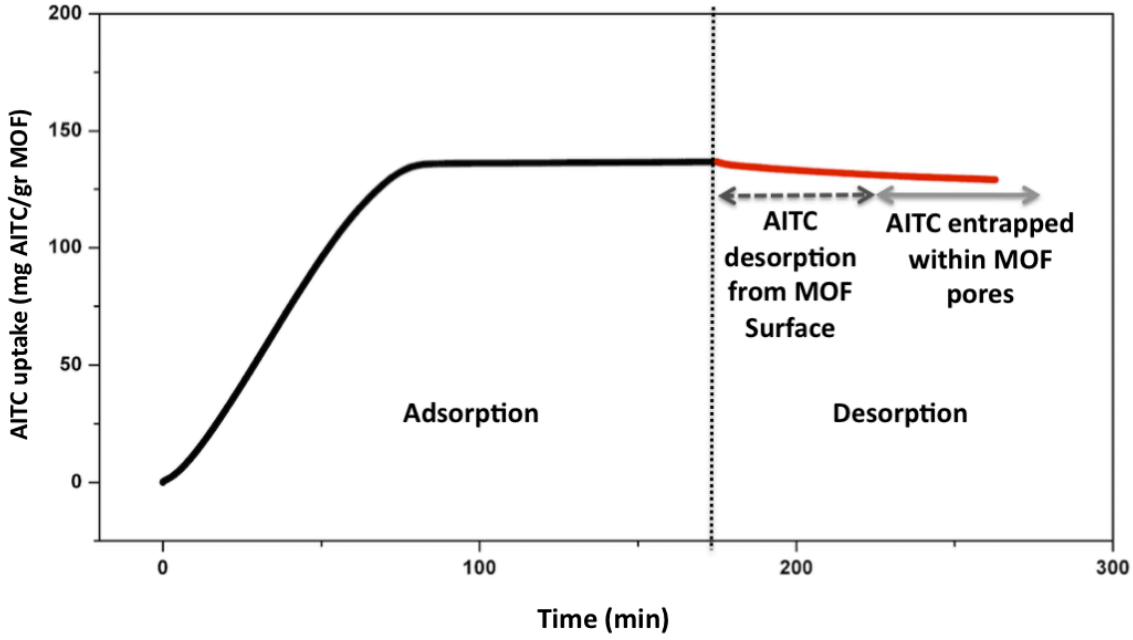

Figure 16. Adsorption-desorption profile of AITC on MOF-74(Zn) microparticles.

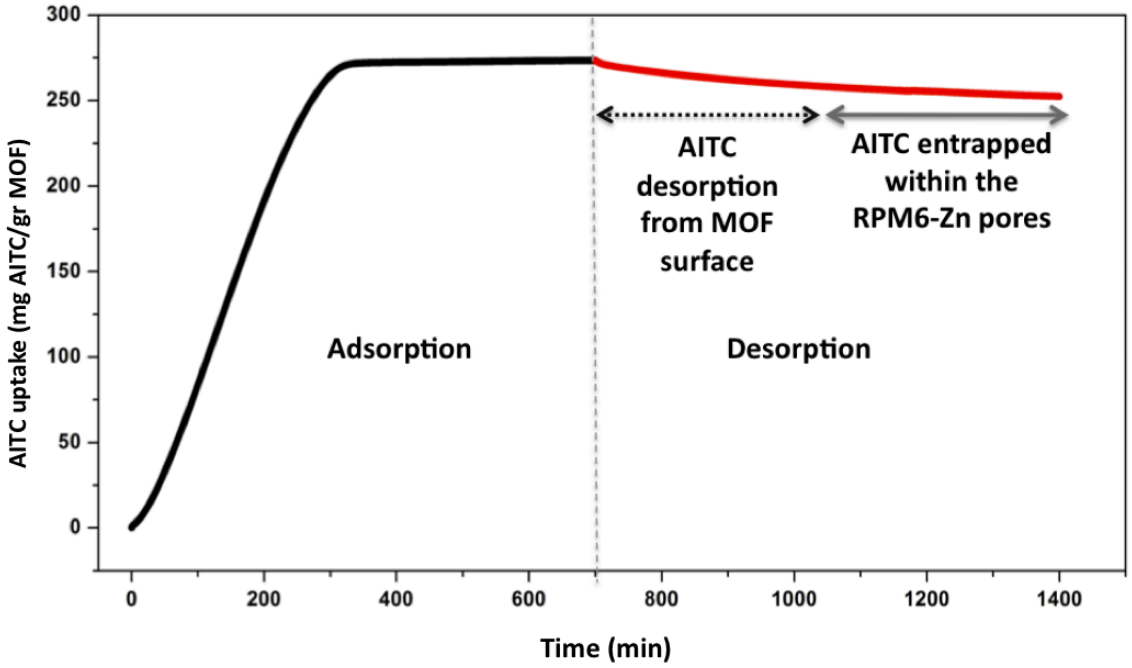

Figure 17. Adsorption-desorption profile of AITC on RPM6-Zn microparticles.

The higher uptake of AITC molecules by HKUST-1 and then RPM6-Zn microparticles can be attributed to their higher BET surface areas (shown in Table 4) and their distinctive structural features. The higher internal surface area of the MOF provides more affinity sites for adsorption of gas molecules, where gas molecules preferentially bind to surfaces in favor of interacting with other gaseous molecules. Therefore, MOFs with higher surface area absorb higher amount of the adsorbate molecules.

On the other hand, although the internal surface areas of MOF-74(Zn) and RPM6-Zn microparticles are in a close range (between 496 and 609 m^2/gr), the uptake of AITC by RPM6-Zn microparticles (27% wt AITC/wt MOF) is almost twice as much as MOF-74(Zn) microparticles (14% wt AITC/wt MOF). This observation implies that factors other than the MOF surface area and pore volume affect the uptake of volatile AITC molecules by these MOFs. As shown in Figure 18, the cage-like pores of HKUST-1

particles and two-fold interpenetrating frameworks of RPM6-Zn particles were able to adsorb and retain higher amounts of AITC molecules within their inner cavities compared to the amounts of AITC adsorbed by the open channel framework of MOF-74(Zn) particles. In other words, the distinctive structural features of HKUST-1 and RPM6-Zn strengthen the interactions between the guest molecules and the MOFs framework through enhancing entrapment and retention of volatile AITC molecules in close proximity of the framework atoms. This reasoning is also aligned with findings from Kesanli et al. (2005), Chun (2008), and Kuppler et al. (2009), indicating that MOFs with distinctive structural features such as cage-like pores and interpenetrating frameworks are superior candidates for sorption and storage of small gaseous molecules.

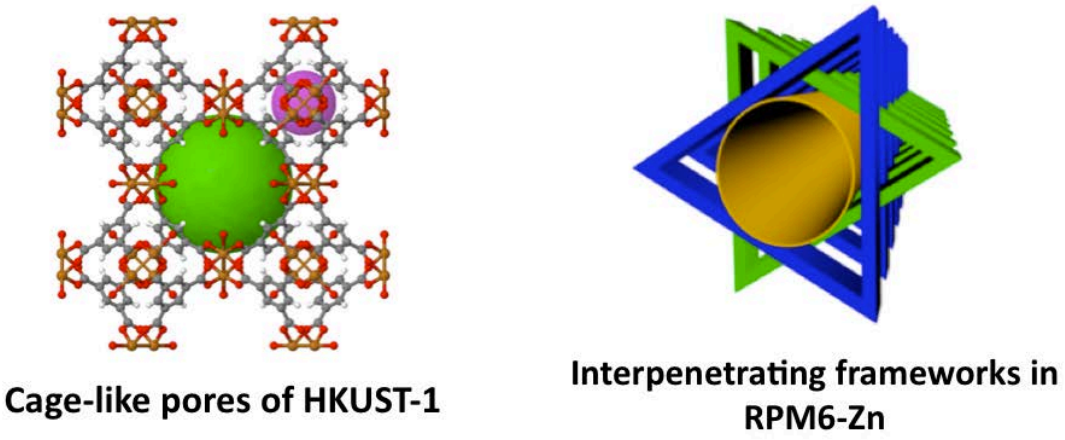

Figure 18. Distinctive structural features that affect AITC adsorption and uptake in (left) HKUST-1 (adapted from www.chemtube3d.com), and (right) RPM6-Zn (adapted from Wang et al., 2016).

Previous studies on few other porous materials including mesoporous silica and brown seaweed (*Saccharina japonica*) showed that both of these porous materials are able to adsorb AITC molecules within their pores (Park et al., 2011; Park et al., 2012;

Siahaan et al., 2014). However, in contrast to the selected MOFs in this research none of these porous materials were able to entrap AITC molecules in their pores upon adsorption resulting in rapid release of AITC due to the relatively large pores (2-7 nanometers) and weak adsorbate-adsorbent interactions between AITC molecules and the pores atoms.

5.3 Controlled Release of AITC

The efficacy of AITC adsorption and later the release profile of AITC molecules by the MOFs microparticles was studied under low (30–35%) and high (95–100%) relative humidity conditions at 24±1 °C (Figure 19). As shown in Figure 20, the non-encapsulated AITC sample displays immediate release of AITC molecules compared to all encapsulated samples. All three MOFs are able to encapsulate and retain more than 90% of encapsulated AITC molecules within their pores at low RH. On the other hand, as Figure 21 shows the release of AITC is triggered in the presence of high RH.

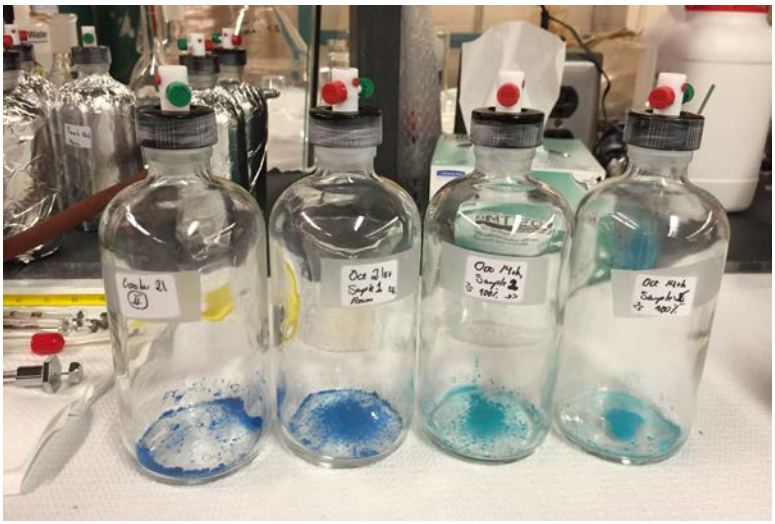

Figure 19. AITC controlled release study under low and high relative humidity at 24±1 °C.

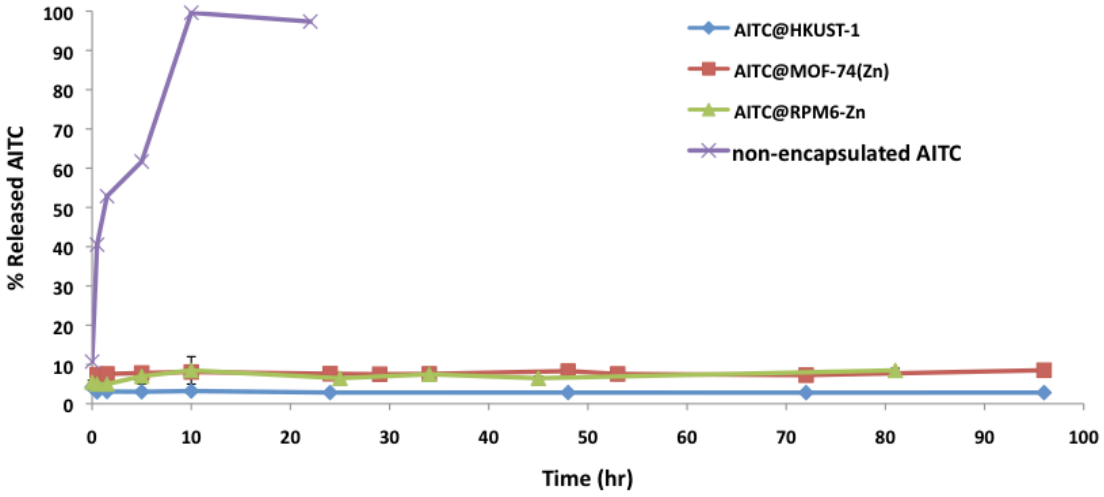

Figure 20. Release profile of AITC from three MOFs at low (30-35%) relative humidity (standard error bars represent STDV/√n).

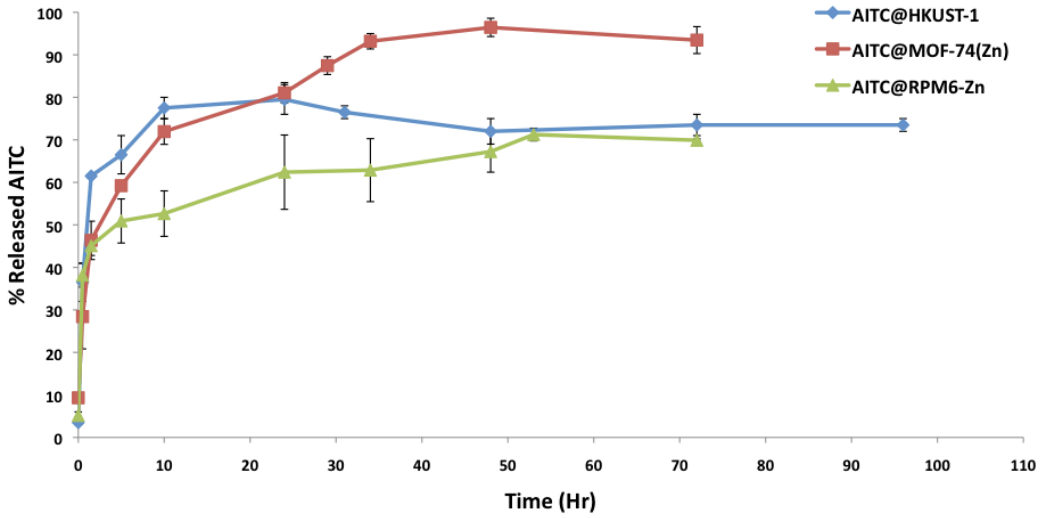

Figure 21. Release profile of AITC from three MOFs at high (90-95%) relative humidity (standard error bars represent STDV/√n).

These results support our hypothesis that the high relative humidity can trigger the release of AITC molecules from these MOFs. Yet, compared to non-encapsulated sample

that immediate release occurred within the first few hours, the release of AITC molecules from all encapsulated trials showed an extended release profiles. An initial rapid release of up to 60% of encapsulated AITC that followed by a slower release period. At the end of the experiment 96, 80, 70% of encapsulated AITC molecules were released from MOF-74(Zn), HKUST-1, and RPM6-Zn, respectively.

As shown in figure 22, similar AITC release profiles were observed in studies conducted by Park, Barton, and Pendelton (2011), Park et al. (2012), and Siahaan et al. (2014) from two different mesoporous silica (MCM-41 and SBA-15) and brown seaweed *Saccharina japonica* microparticles. However, using MOF microparticles as delivery systems has the advantage that release of AITC can be triggered by an external stimulus, which is exposure to high RH, while the releases from both seaweed powder and mesoporous silica were passive and controlled by the pore size only.

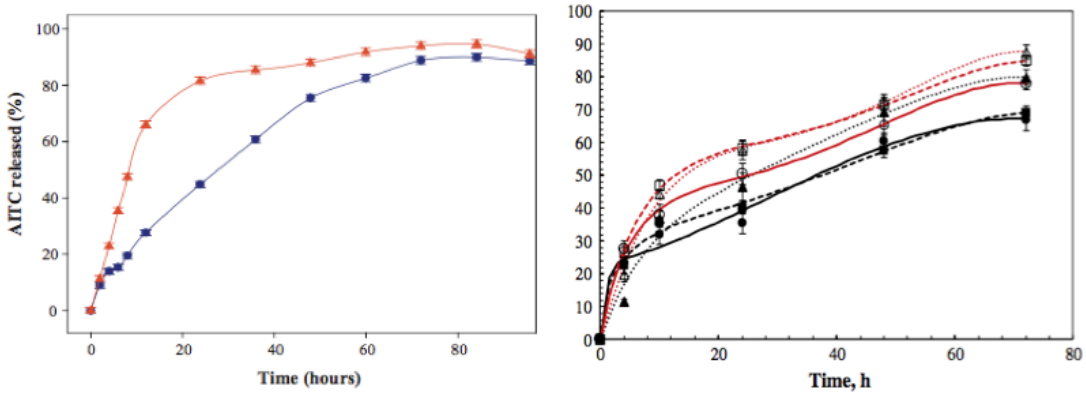

Figure 22. (Left) release of AITC from silica (blue square: MCM-41, orange triangle: SBA-15) adapted from Park et al (2011), (right) release profile of AITC vapors from raw and de-oile *S. japonica* (• 500 µm raw *S. japonica*; ■ 710 µm raw *S. japonica*; black triangle 900 µm raw *S. japonica*; red circle: 500 µm de-oiled *S. japonica*; red square 710 µm de-oiled *S. japonica;* red triangle 900 µm de-oiled *S. japonica* adapted from Siahaan et al., 2014.

According to findings of Park et al. (2012), the early moderately high release rate of volatile AITC molecules from mesoporous silica within the first 10 hrs of the release generated a rapid lethal dose of antimicrobial AITC against selected food-borne bacteria and fungi that successfully inhibited their growth. Besides, the extended slow release of AITC led to distinct reduction in viable counts of each pathogen. Also Inouye, Takizawa, and Yamaguchi (2001) reported that rapid evaporation of 14 essential oils when applied at sufficient concentrations is more effective than their slow evaporation to inhibit the growth of *Streptococcus* pathogenic bacteria.

While 96% of encapsulated AITC released from MOF-74(Zn), the observation that 70–80% of encapsulated AITC molecules in HKUST-1 and RPM6-Zn microparticles are released can be explained through the effects of two factors. First, moderate disruptions of 3D frameworks of RPM6-Zn particles by water molecules that substitute the organic ligands in coordination sites can hinder the release of entrapped AITC molecules. Second, formation of strong bonds between more-polar isothiocyanate end (-N=C=S) of AITC molecules and the available charged atoms of water clusters attached to the exposed coordination sites of RPM6-Zn and unsaturated metal centers (UMC) of HKUST-1 microparticles that may prevent some of the encapsulated AITC molecules from release. These water clusters when merge together can also hinder the release of some of the residual AITC molecules from the pores before all encapsulated AITC molecules can escape from the MOF cavities to the headspace.

It is worth mentioning that although MOF-74(Zn) releases the highest percentage (96%) of the encapsulated AITC from its open pores, the amounts of AITC that released from this MOF was the lowest compared to the other two MOF due to its lower AITC

loading capacity (Figure 23). Based on the loading capacities and percentage of release, the final amounts of AITC released from these three MOFs at high RH is in the order of HKUST-1>RPM6-Zn>MOF-74(Zn).

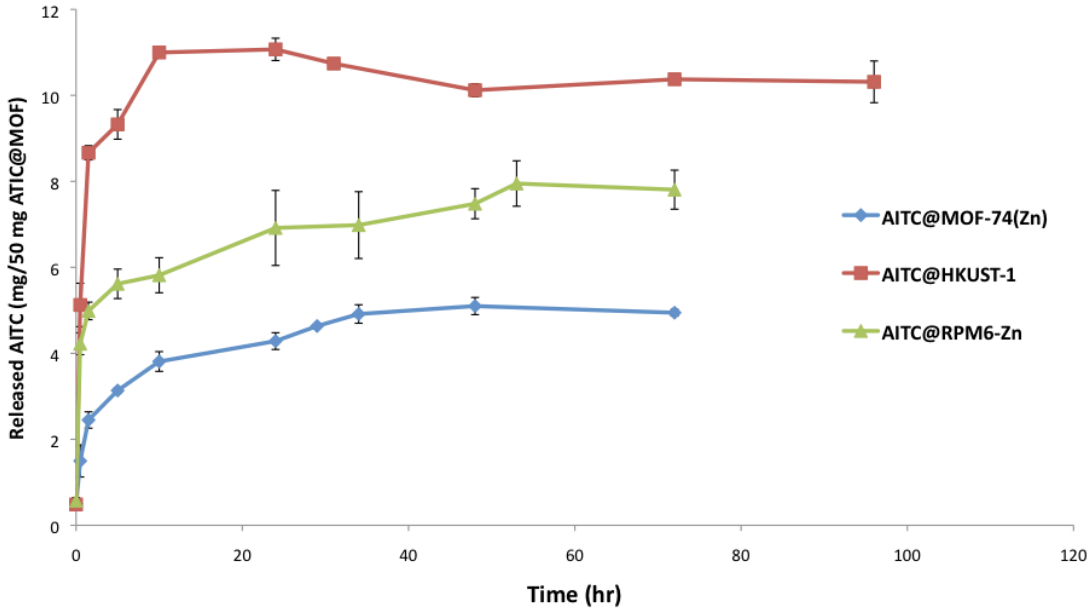

Figure 23. Amounts of AITC released from the three MOFs at high (95-100%) relative humidity (standard error bars represent STDV/√n).

The effect of temperature on AITC release from RPM6-Zn microparticles was also investigated at high RH. As shown in Figure 24, increasing temperature increases both rate and amounts of ATIC release from RPM6-Zn microparticles. At 6 °C that mimics the refrigerator temperature, 90% of the entrapped AITC molecules remained inside the pores, while almost all the entrapped AITC molecules were released from the MOF at 35 °C in a very short period of time. A faster AITC release also was observed by Seo et al (2012) at 25 °C than at 4 °C. We attributed these results to the effects of higher temperatures on increasing the diffusion rates and the reaction energy among the molecules that leads to the faster release of AITC molecules. Given that abusive high

temperatures along with the presence of high RH will accelerate the microbial growth, the obtained results at 24 and 35 °C will ensure the release of AITC soon enough and to sufficient quantity to the headspace of the food package to keep the packed food from developing any potential pathogenic or spoilage contamination during its shelf life.

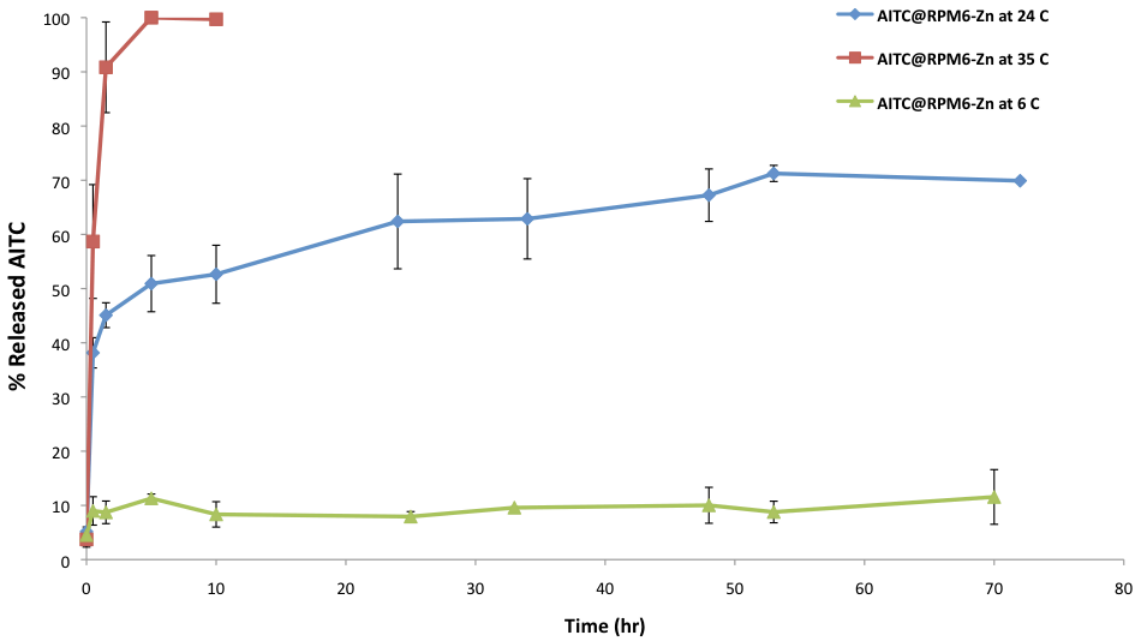

Figure 24. Release profile of AITC from RPM6-Zn particles at high (95-100 %) relative humidity conditions and three different temperatures.

Involved mechanism- Diffusion and interaction energy (kT) are the main underlying mechanisms in which temperature affects the release kinetics of volatile AITC molecules from RPM6-Zn microparticles at high relative humidity conditions.

Release of AITC molecules requires the structural transformation of RPM6-Zn from a 3D crystalline structures to a nonporous structure, which is accessible through diffusion of water vapor molecules from the headspace to the MOFs pores particles and eventually the metal-ligand sites. Diffusivity of water vapor molecules in both headspace and the

microporous crystalline frameworks of RPM6-Zn particles depend on the diffusion coefficient (*D*) of water vapors in both media. As stated in equations 1 based on Chapman-Enskog theory, temperature directly affects the magnitude of diffusion coefficient (*D*), thereby higher temperatures increase the diffusivity of water vapors in the headspace.

$$D = \frac{1.858 \times 10^{-3} T^{3/2} \sqrt{1/M_1 + 1/M_2}}{p\sigma_{12}^2 \Omega}$$ Equation 1.

Where *D* is the diffusion coefficient of water vapors in the headspace air (m^2/s), T is the absolute temperature (K), M_1 and M_2 are molar mass (g/mol) of water vapor and air, *p* is pressure (atm), σ_{12} is the average collision diameter ($\sigma_{12}=½(\sigma_1+\sigma_2)$), and Ω is a temperature-dependent collision integral (dimensionless).

Also based on Equation 2 the diffusivity of water vapors within the microporous structure also is diffusion coefficient dependent, which in turn relies on the temperature (Grathwohl, 1998).

$$D_e = \frac{D\varepsilon_t \delta}{\tau}$$ Equation 2.

Where D_e is the effective diffusion coefficient of water vapor in porous media (m^2/s). *D* is the diffusion coefficient of gas filling the pores (m^2/s), ε_t is the porosity[6] available for the transport (dimensionless), δ is the constrictivity[7] (dimensionless), and τ is the

[6] Porosity is a measure of the void or empty spaces in a material and is a fraction of the volume of voids over the total volume.
[7] Constrictivity is used to describe transport process in molecular diffusion in porous media and depends on the ratio of the diameter of the diffusing particle to the pore diameter.

tortuosity[8] (dimensionless). Further information regarding transport diffusivity of AITC molecules into and out of microporous RPM-Zn materials can be obtained through application of techniques such as high temporal and spatial resolution IR microimaging and interference (IF) microscopy.

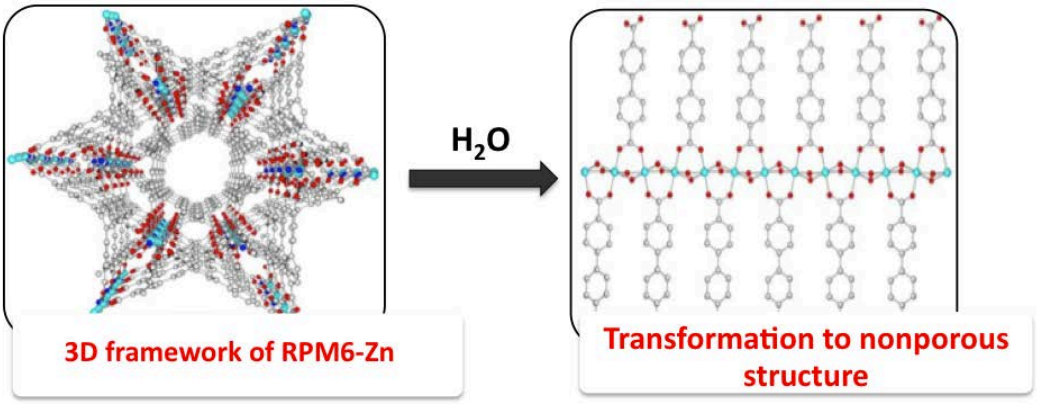

Figure 25. Structural breakdown of RPM6-Zn particles by water molecules (adapted from Wang et al., 2016 with modifications).

As mentioned earlier, interaction energy is the second underlying mechanism through which temperature affects the release rate of AITC molecules from RPM6-Zn particles. Interaction energy (kT)[9] is the amount of heat required to increase the thermodynamic entropy of a system. As a result, higher temperatures provide the required interaction energy for water vapor molecules to compete for the ligand sites (specifically Zn-N bonds) and thereby break Zn-N coordination bonds to form new Zn-O bonds (Figure 25).

[8] Tortuosity is a property of curve being twisted and is commonly used to describe diffusion in porous media. It is the ratio of the length of the curve (L) to the distance between the ends of it (C): $\tau = L/C$

[9] Where k is the Boltzmann's constant (J/K) and T is the temperature (K). In physics, kT is used as a scale factor for energy values in molecular scale.

5.4 Morphological Study of MOFs

SEM micrographs show that the morphology of samples kept at low RH remained almost intact with well-defined structures and smooth surfaces (Figures 26a, c, e). In contrast, samples kept at high RH show minor to major changes in their form and structure. HKUST-1 and MOF-74(Zn) show small cracks on surfaces, although they still maintain their overall integrity and forms (Figures 26b, d). In contrast to HKUST-1 and MOF-74(Zn), RPM6-Zn went through major structural transformation when exposed to high RH (Figure 26f). As discussed earlier, the appearance of rough and multilayer structure can be explained through major structural changes of RPM6-Zn particles from microporous 3D framework to 1D coordination polymer chains.

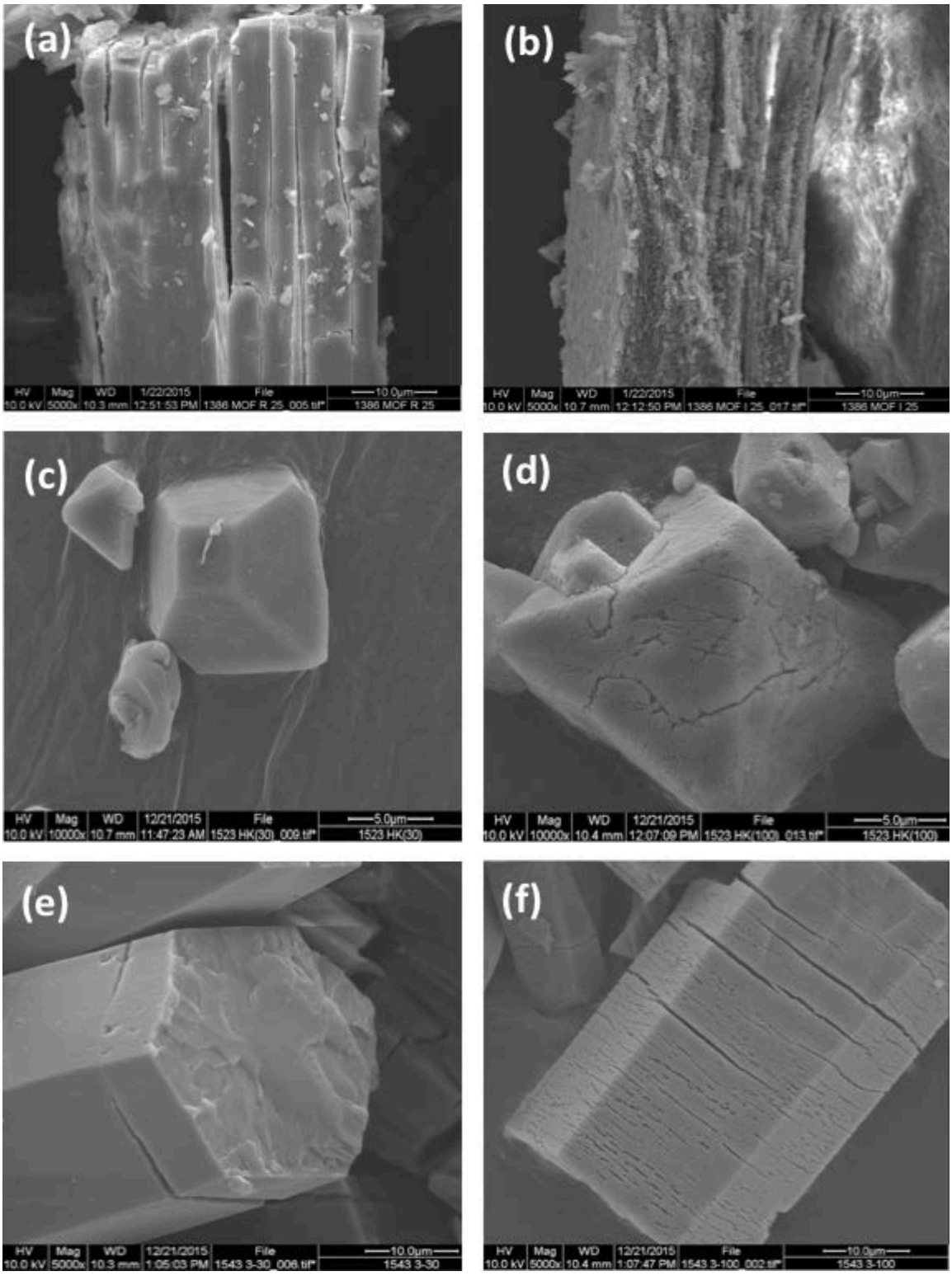

Figure 26. Scanning electron micrographs of: (a) RPM6-Zn particles kept at low (30-35) %RH; (b) RPM6-Zn micro particles kept at high (95-100) % RH; (c) HKUST-1 particles kept at low (30-35) %RH; (d) HKUST-1 micro particles kept at high (95-100) % RH;(e) MOF-74(Zn) particles kept at low (30-35) % RH; (f) MOF-74(Zn) particles kept at high (95-100) % RH.

The destructive effect of water molecules on RPM6-Zn 3D microporous structure, which results in major structural transformation, is shown in Figure 27 (a and b). Its rough and multilayer appearance is attributed to the transformation from a 3D framework to a nonporous structure by water molecules.

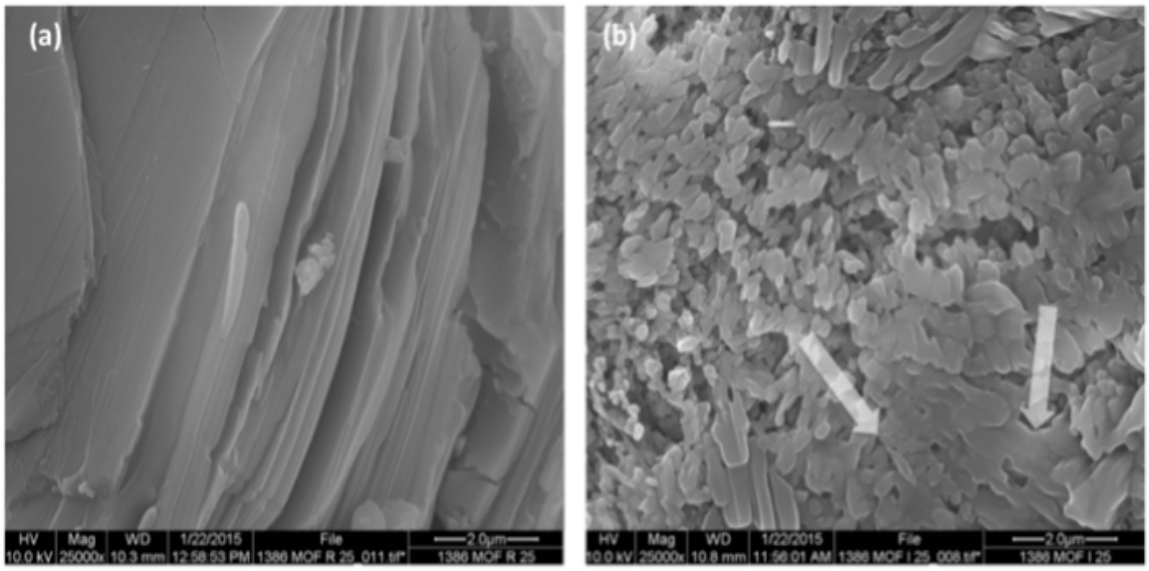

Figure 27. Scanning electron micrographs of RPM6-Zn microparticles at 24 C under (a) low (30-35) %RH, and (b) under high (90-95) %RH.

While results from SEM images suggest major structural changes in 3D framework of RPM6-Zn when exposed to high moisture content conditions, further evidence of structural changes was provided through TEM study. As illustrated in Figure 28, 29, and 30, the samples kept at low moisture content conditions show regular and dense structure, while the samples exposed to high relative humidity conditions lack dense and well-defined structure, which implies the breakdown of 3D framework. Smooth and regular outline of samples kept at low relative humidity conditions compared to the irregular and rough outline of samples kept at high moisture content conditions

support our hypothesis that the 3D frameworks of RPM6-Zn undergoes gradual breakdown when exposed to high moisture content conditions, thereby allow the release of entrapped AITC molecules within its pores. TEM micrographs also show that the regular and well defined outline of these two MOFs remain almost unchanged at both high and low RHs.

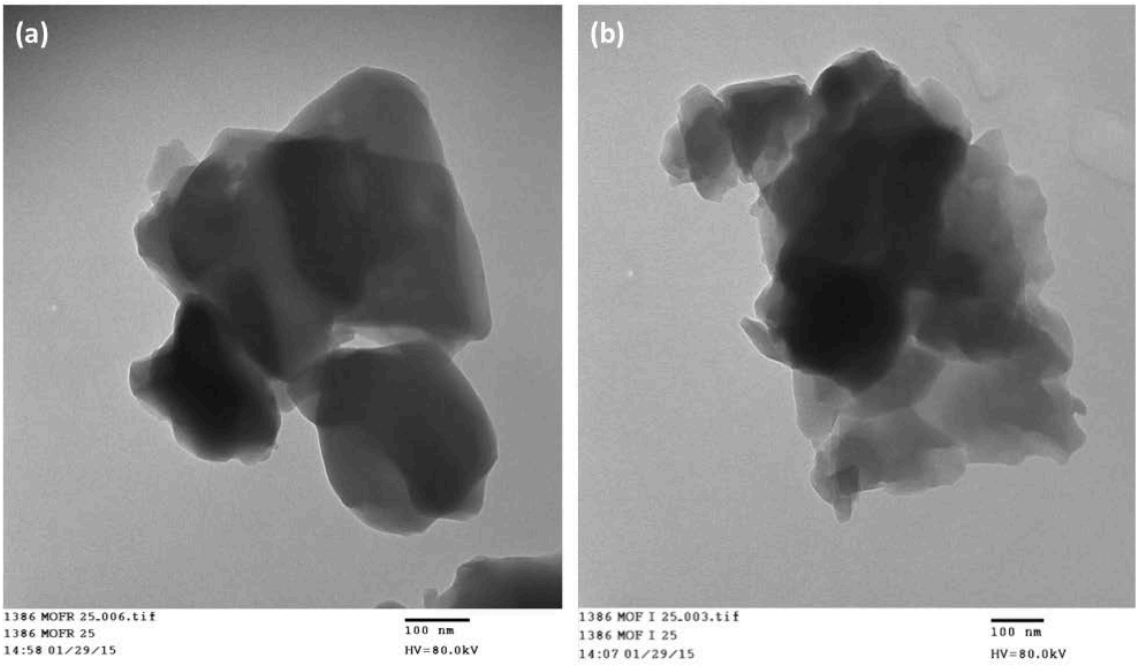

Figure 28. Transmission electron micrographs of RPM6-Zn microparticles kept at (a) low (30-35) %RH, and (b) high (90-95) %RH.

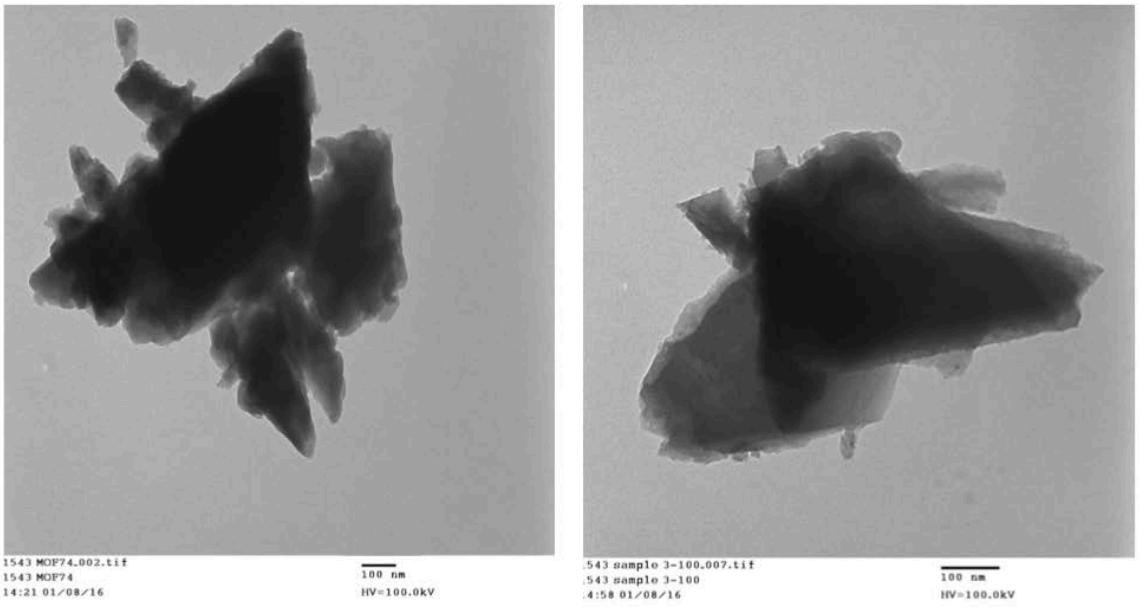

Figure 29. Transmission electron micrographs of MOF-74(Zn) microparticles kept under (left) low (30-35) %RH, and (right) high (95-100) %RH.

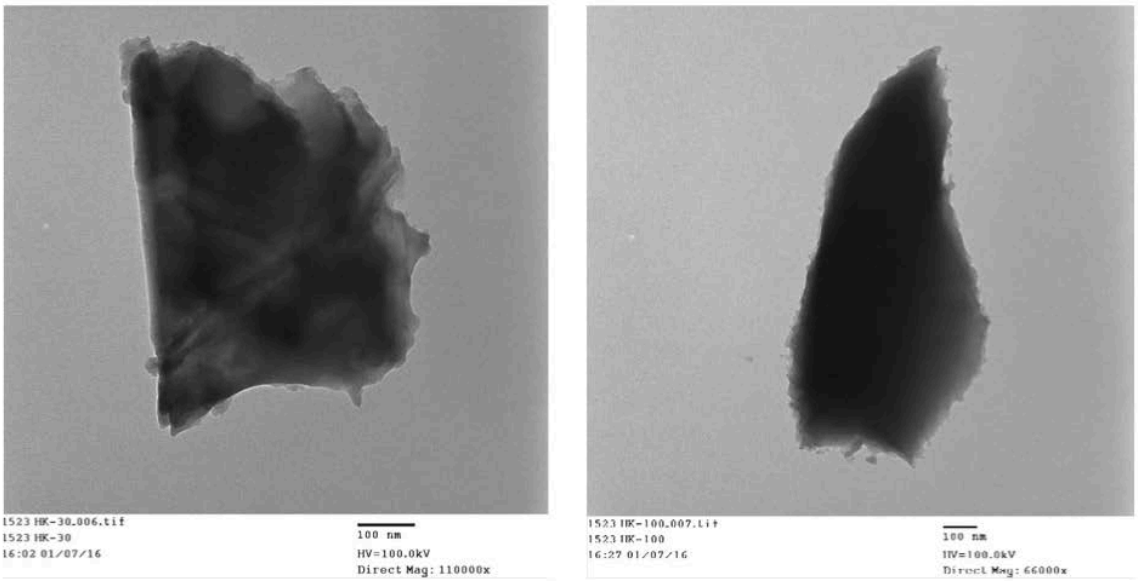

Figure 30. Transmission electron micrographs of HKUST-1 microparticles kept under (left) low (30-35) %RH, and (right) high (90-95) %RH.

5.5 Crystalline Properties of MOFs

Although the AITC release from RPM6-Zn can be explained by the structural breakdown observed by SEM and TEM imaging, the mechanism responsible for the AITC release from HKUST-1 and MOF-74(Zn) at high RH remains unknown. Hence XRPD analysis was conducted to determine whether breakdown occurred at the crystalline structure. Presence of crystalline structure at high RH means that although minor structural deformation in the form of small cracks occurred in these MOFs, water molecules did not cause the MOF crystalline structure to breakdown through organic ligands substitution at metal-ligand coordination sites in the two MOFs that leads to the AITC release.

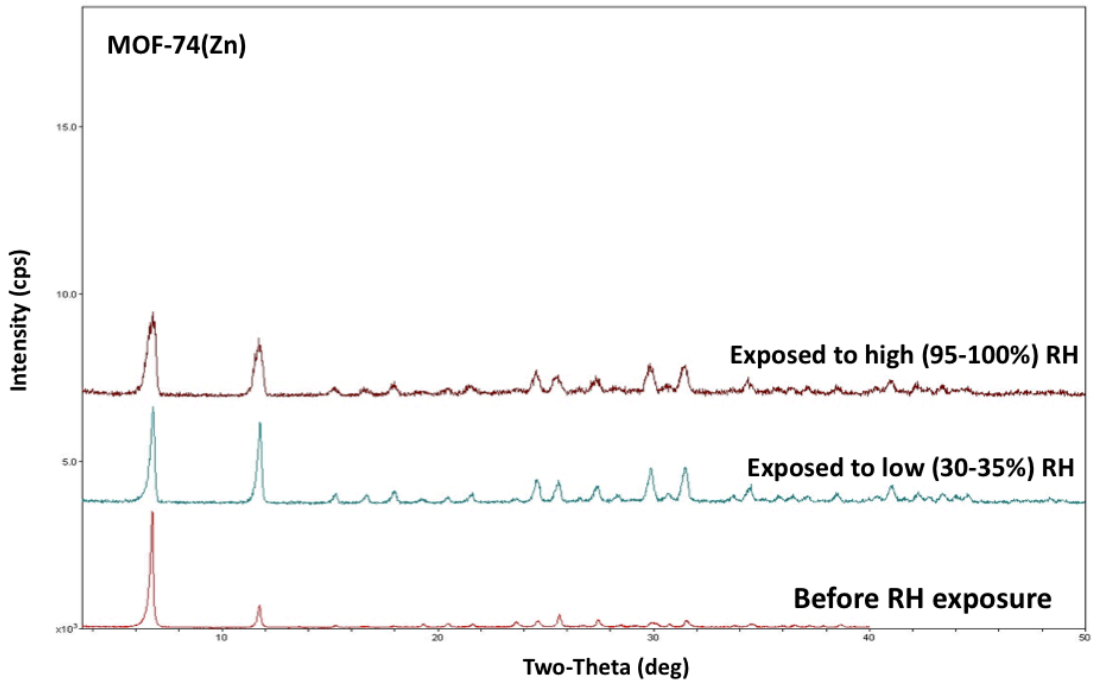

Figure 31. XRPD pattern of MOF-74(Zn) before RH exposure (red, bottom), after exposure to low (30-35%) RH (green, middle), and after exposure to high (95-100%) RH (brown, top).

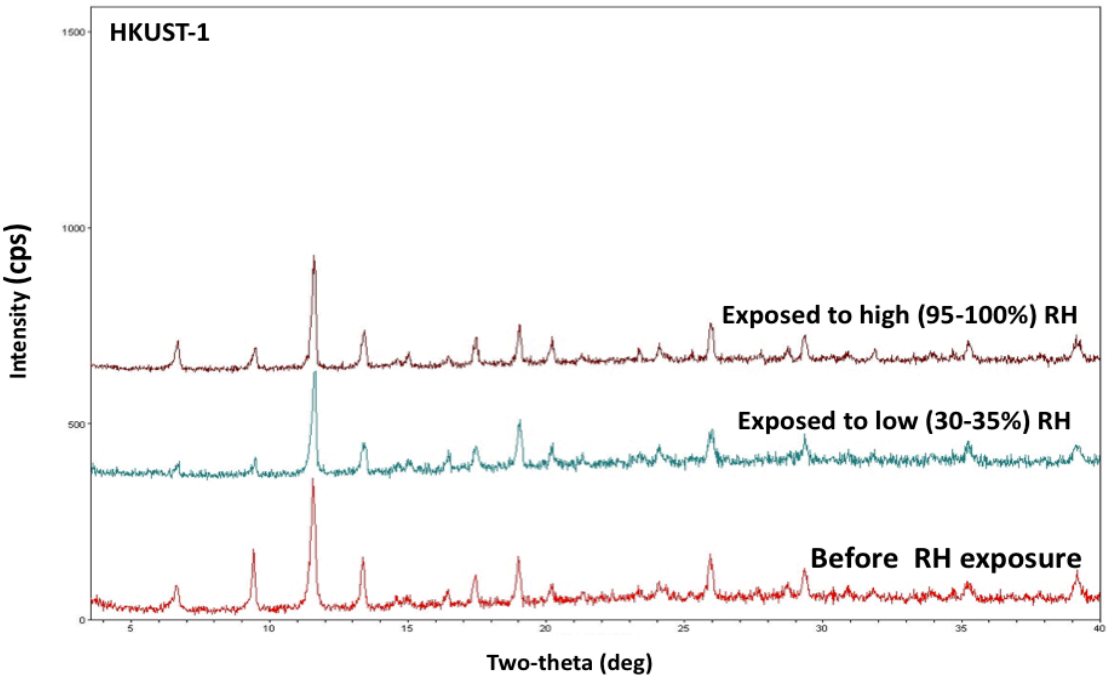

Figure 32. XRPD patterns of HKUST-1before RH exposure (red, bottom), after exposure to low (30-35%) RH (green, middle), and after exposure to high (95-100%) RH (brown, top).

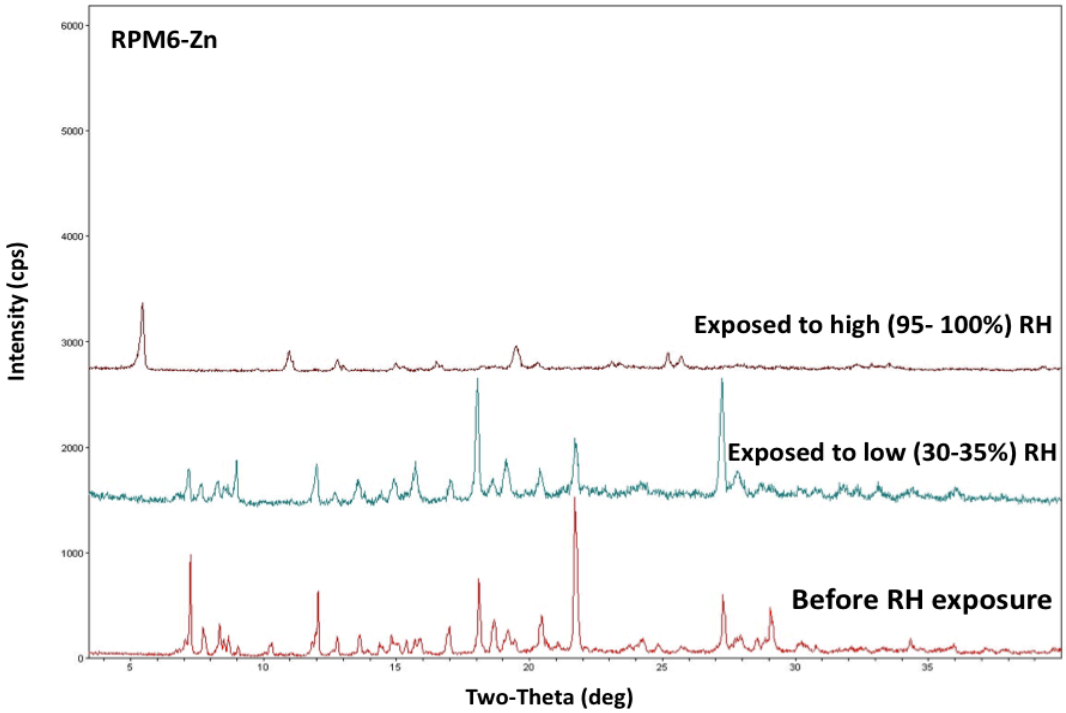

Figure 33. XRPD patterns of RPM6-Zn before RH exposure (red, bottom), after exposure to low (30-35%) RH (green, middle), and after exposure to high (95-100%) RH (brown, top).

Figures 31, 32 and 33 show that under low RH conditions, X-ray patterns of the three MOFs were almost unchanged compared to those before RH exposure, indicating their highly ordered crystalline structures were maintained. When exposed to high RH, the X-ray patterns of HKUST-1 and MOF-74(Zn) were still unchanged, but the X-ray pattern of RPM6-Zn was changed substantially indicating significant loss of its highly order structure. These results along with findings from SEM and TEM micrographs confirmed that AITC release from RPM6-Zn is driven by transformation of a 3D network structure to a nonporous structure. As discussed in Wang et al. (2016), the substitution of organic ligands mainly 4,4'-azobispyridine pillar ligands by water molecules at metal-ligand coordination sites (Zn–N) leads to the MOF structural breakdown and release of entrapped AITC molecules.

Based on the results from SEM, TEM, and XRPD analyses, we propose that the replacement of entrapped less-polar AITC molecules by polar water vapor molecules within the highly polar pores and channels of HKUST-1 and MOF-74(Zn) is the driving force causing the AITC release from the two MOFs (Figure 34). As shown in Figures 11 and 12, the large hydrophilic pores and unsaturated metal centers consist of Cu_2(OOC-) paddlewheel secondary building unit (SBU) in HKUST-1, and hydroxyl groups of organic ligands in MOF-74(Zn) open channels are the hydrophilic attraction sites for water molecules. The adsorbed water molecules act as the main affinity sites for adsorption of other water molecules through hydrogen bonding, which ultimately result in the formation of small water clusters that force the exit of AITC molecules from the pores and channels of the two MOFs. However, when these small water clusters grow larger and merge with neighboring water clusters quickly, they can in fact hinder the

release of some of the residual AITC molecules from the pores before the full release of encapsulated AITC molecules occur. The results of X-ray powder diffraction also confirm that metal-O coordination sites in HKUST-1 and MOF-74(Zn) are more water stable than metal-N bonds in RPM6-Zn, making the two MOFs structurally more stable to high RH than the RPM6-Zn particles.

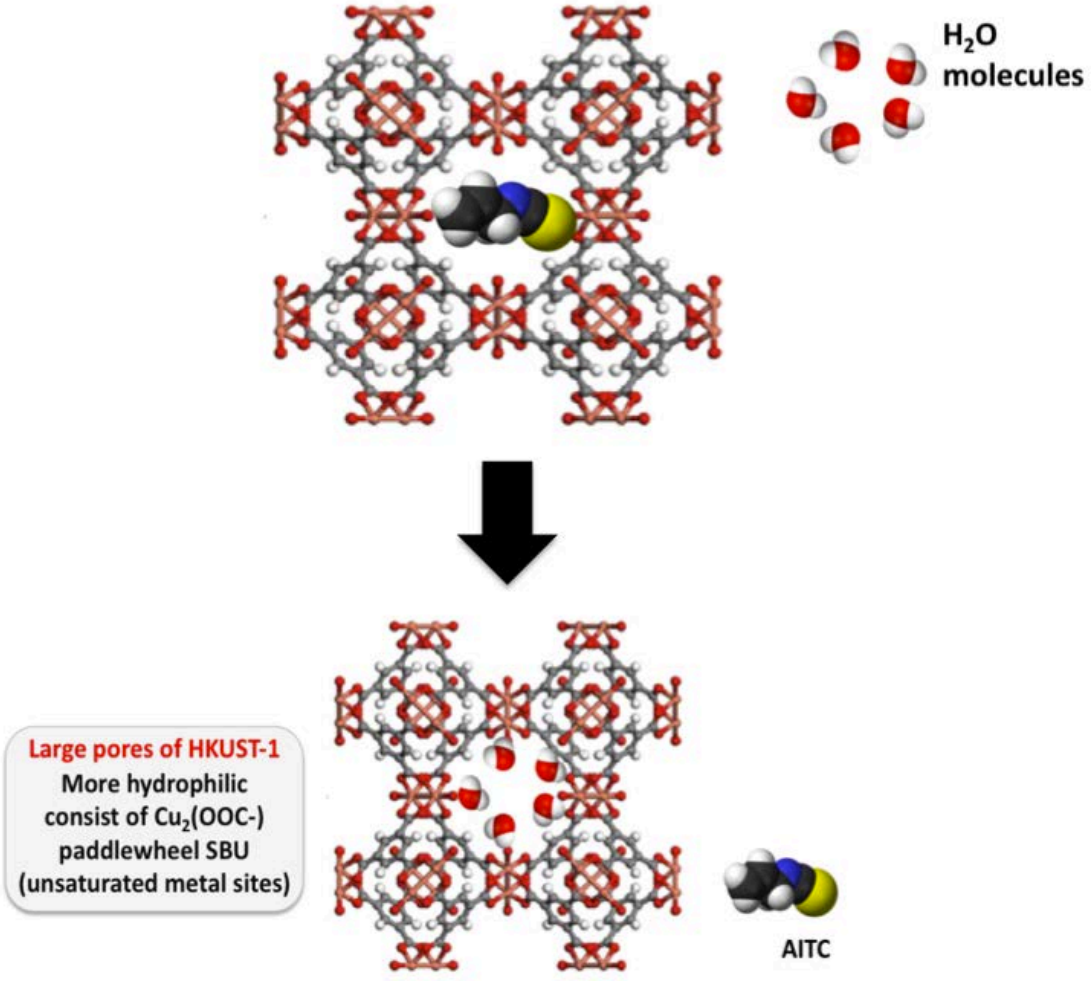

Figure 34. Diagram of proposed release mechanism of encapsulated AITC from HKUST-1 (and MOF-74(Zn) pores.

6. Conclusion

This research investigated the potential application of metal-organic frameworks as novel delivery systems for adsoption and controlled release of volatile AITC antimicrobial molecules. The three MOFs were able to encapsulate AITC molecules with loadings ranging between 130 and 400 mg AITC/gr MOF. Exposure to 30–35% RH resulted in only 10% AITC release, with the remaining 90% still encapsulated inside the pores and channels of the MOFs. But exposure to 95–100% RH resulted in AITC release ranging between 70 and 96%. This finding support our hypothesis that water vapor at high concentration can act as an effective trigger to release AITC molecules from these MOFs.

SEM, TEM, and XRPD analyses show that exposure to low RH (30–35%) did not cause structural changes in all three MOFs. While exposure to high RH (95–100%) caused a major structural change in RPM6-Zn, it caused only minor structural changes in HKUST-1 and MOF-74(Zn). This observation suggests that the major structural change caused by substitution of metal-nitrogen bonds at coordination sites with metal-oxygen(water) is the main factor affecting the AITC release from RPM6-Zn. However, the factor(s) affecting the AITC release from HKUST-1 and MOF-74(Zn) are less obvious. This research propose that polar water vapor molecules replace less-polar entrapped AITC molecules entrapped inside the highly polar cavities of HKUST-1 and MOF-74(Zn) particles forcing the release of AITC molecules from the two MOFs.

This study provides encouraging results to indicate that the application of MOFs as novel delivery systems for encapsulation and controlled release of AITC molecules using high relative humidity as the external trigger is technically feasible. For commercial applications, these AITC-MOFs particles can be packed in sachets permeable

to both AITC and water vapors, sealed and placed inside the food package (Otoni, Espitia, Avena-Bustillos, and McHugh, 2016). Upon the water vapor triggered release, volatile AITC molecules from the MOFs will diffuse to the food surfaces via the package headspace to inhibit microbial growth and extend shelf life. Designing the sachet with the proper dimensions and constructing it with a material with proper AITC and H_2O permeability make a desired release rate achievable. Gonçalves, Pires, Soares, and Araújo (2009), Pires, Soares, Andrade, Silve, Camilloto, and Bernardes (2009), Soe, Bang, Kim, Beuchat, Cho, and Ryu (2012), and Otoni, Soares, Silva, Medeiros, and Junior (2014) also reported the development of antifungal and antibacterial AITC sachets for peanuts, cottage cheese, mozzarella cheese, and fresh spinach preservation suggesting the application of these AITC emitting sachets can be technically practical. We believe this research could make contribution to improve safety, storage, and transportation shelf life of fresh and high moisture content packaged foods.

7. Recommendations for Futures Studies

The results of this study revealed that the potential application of the three selected MOFs as novel delivery systems for adsoption and controlled release of volatile AITC molecules is technically feasible. Given the outcomes of this research, some of the prospective areas for further investigation are as following:

- Considering the two proposed mechanisms of AITC release from the selected MOFs, a closer look to better understand the interaction of water molecules within these materials is suggested. Currently, few studies investigating water adsorption by MOFs are available, and further research is required to understand the behavior of water molecules both in liquid and vapor phases within these structures, and the relationship between the MOFs structural properties and their water adsorption characteristics. Ultimately how water adsorption affects the structural properties of MOFs over time in specific stability of MOFs frameworks, their inner surface area, and adsorption properties would be beneficial in predicting their behavior on real-life conditions and for practical applications.
- Given that most applications of MOFs including gas storage, separation, and delivery agent of bioactive compounds involve adsorption of the guest molecules and their interaction within MOFs cavities, further investigation on the role of potential unknown factors affecting loading and retention of these guest molecules is suggested.
- Considering the potential application of MOF as carriers and delivery systems for bioactive (or additives) agents for food industry application, synthesis and tuning a

novel series of MOF with suitable pore size and structural components for application in food systems can be an interesting field of endeavor for researchers.

8. Cited Works

An J., Geib S. J., Rosi N. L. Cation-triggered drug release from a porous zinc-adeninate metal-organic framework. *J. Am. Chem. Soc*. 2009. (131) 8376-8377.

Appendini P., Hotchkiss J. H. Review of antimicrobial food packaging. *Innovative Food Science & Emerging Technologies*. 2002. (3) 113-126.

Aytac Z., Dogan S. Y., Tekinay T., Uyar T. Release and antibacterial activity of allyl isothiocyanate/β-cyclodextrine complex encapsulated in electrospun nanofibers. Journal of colloids and Surfaces. 2014. (120) 125-131.

Batten S. R., Champness N. R., Chen X., Garcia-Martinez J., Kitagava S., Öhrström L., O'Keeffe M., Suh M. P., Reedijk J. Terminology of metal-orgainc frameworks and ccordination polymers (IUPAC recommendation 2013). *Pure Appl. Chem*. 2013. 85(8) 1715-1724.

Britt, D., Furukawa, H., Wang B., Glover, T., & Yaghi, O. M. Highly efficient separation of carbon dioxide by a metal-organic framework replete with open metal sites. *Proceedings of the National Academy of Sciences*, 2009. 106(49), 20637-20640.

Castillo J. M., Vlugt T. J. H., Calero S. Understanding water adsorption in Cu-BTC metal-organic frameworks. *J. Phys. Chem*. 2008. 112(41) 15934-15939.

Cejpek K., Valusek J., Velisek J. Reactions of allyl isothiocyanate with alanine, glycine, and several peptides in model systems. *J. Agric. Food Chem*. 2000. (48) 3560-3565.

Chacon P. A., Buffo R. A., Holley R. A. Inhibitory effects of microencapsulated allyl isothiocyanate (AITC) against *Escherichia coli* O157:H7 in refrigerated, nitrogen packed, finely chopped beef. *International Journal of Food Microbiology*. 2006. (107) 231-237.

Chen C., Ho C. T. Thermal degradation of allyl isothiocyanate in aqueous solutions. *J. Agric. Food Chem*. 1998. (46) 220-223.

Chun, H. Low-level self-assembly of open framework based on three different polyhedra: metal-organic analogue of face-centered cubic dodecaboride. *Journal of American Chemical Society,* 2008. (130) 800-801.

Chui S., Lo S., Charmant J., Orpen A., & Williams A. A chemically functionalizable nanoporous material. Science. 1999. (283) 1148-1150.

Dai R., Lim L. Release of allyl isothiocyanate from mustard seed meal powder. *Journal of Food Science*. 2014. 79(1) E47-E53.

Dias M. V., Soares N. F., Borges S. V., Sousa M. M., Nunes C. A., Oliveira I. N. Use of allyl isothiocyanate and carbon nanotubes in an antimicrobial film to package shredded, cooked chicken meat. *Food Chemistry*. 2013. (141) 3160-3166.

Delaquis O. J., Mazza G. Antimicrobial properties isothiocyanates in food preservation. *Food Technology*. 1995. 49(11) 73-84.

Delaquis P. J., Sholberg P.L. Antimicrobial activity of gaseous allyl isothiocyanate. *Journal of food protection*. 1997. 60 (8) 943-947.

Depree J. A., Savage G. P. Physical and flavor stability of mayonnaise. *Trends in Food Science & Technology*. 2001. (12) 157–163.

Dias, M. V., Soares, N. F., Borges, S. V., Sousa, M. M., Nunes, C. A., & Oliveira, I. N. Use of allyl isothiocyanate and carbon nanotubes in an antimicrobial film to package shredded, cooked chicken meat. *Food Chemistry*. 2013. (141) 3160-3166.

Eddaoudi M., Li H., Yaghi O. M. Highly porous and stable metal-orgnic framworks: structure design and sorption properties. *J. Am. Chem. Soc*. 2000. (122) 1391-1397.

Eddaoudi M., Moler D., Li H., Chen B., Reineke T., O' Keeffe M., Yaghi O. M. Modular Chemistry: secondary building units as a basis for the design of highly porous and robust metal-organic carboxylate frameworks. *Accounts of Chemical Research*. 2001. 34(4), 319-330.

Frankel F., Priven. M., Richard E., Schweinshault C., Tongo O., Webster A., Barth E., Slejzer, K., & Edelstein S. Health Functionality of Organosulfides: A Review. *International Journal of Food Properties*. 2016. (19) 537–548.

Frost H., Düren T., Snurr R. Q. Effects of surface area, free volume, and heat of adsorption on hydrogen uptake in metal-organic frameworks. *J. Phys. Chem*. 2006. (110) 9565-9570.

Furia T. E., Bellanca N. Fenaroli's handbook of flavor ingredients. Volume1. 2nd Edition. Cleveland. The chemical rubber co., 1975. P188.

Glover, T. G., Peterson, G. W., Schindler, B. J., Britt, D., & Yaghi, O. MOF-74 building unit has a direct impact on toxic gas adsorption. *Chemical Engineering Science*. 2011. (66) 163-170.

Goi H., Inouye S., Iwanami Y. Antifungal activity of powdery black mustard, powdery wasabi (Japanese horseradish), and allyl isothiocyanate by gaseous contact-Antifungal activity of plant volatiles. *Journal of Antibacterial and Antifungal Agents*. 1985. 13(5) 199-204.

Gonçalves, M. P. J. C., Pires, A. C. S., Soares, N. F. F., & Araújo, E. A. Use of allyl isothiocyanate sachet to preserve cottage cheese. *Journal of Food service.* 2009. (20) 275–279.

Grathwohl P. Diffusion in natural porous media: contaminant transport, sorption/desorption and dissolution kinetics. Springer science+business media, LLC. New York. 1998. pp 205.

Greathhouse J. A., Allendorf M. D. The interaction of water with MOF-5 simulated by molecular dynamics. *J. Am. Chem. Soc*. 2006. (128) 10678-10679.

Haynes W. M. CRC handbook of chemistry and physics. 91st ed. Boca Raton, FL. CRC press Inc. 2010-2011. pp 3-12.

Horcajada et al. Porous metal-organic-framework nanoscale carriers as a potential platform for drug delivery and imaging. *Nature Materials*. 2010. (9) 172-178.

Horcajada P., Gref R., Baati T., Allan P. K., Maurin G., Couvreur P., Férey G., Morris R. E., Serre C. Metal-Organic Frameworks in biomedicine. *Chemical Reviews*. 2012. (112) 1232-1268.

Huang L. Wang H., Chen J., Wang Z., Sun J., Zhao D., Yan Y. Synthesis, morphology control, and properties of porous metal-organic coordination polymers. *Microporous and Mesoporous Materials*. 2003. (58) 105-114.

Hyldgaard M., Mygind T., Meyer L. R. Essential oils in food preservation: mode of action, synergies, and interactions with food matrix components. *Frontiers in Microbiology*. 2012. (3) 1-23.

Inouye S. Goi H., Miyauchi K., Muraki S., Ogihara M., Iwanami Y. Inhibitory effect of volatile constituents of plants on the proliferation of bacteria- Antibacterial activity of plant volatiles. *Journal of Antibacterial and Antifungal Agents*. 1983. 11(1) 609-615.

Inouye S., Takizawa T., Yamaguchi H. Antibacterial activity of essential oils and their major constituents against respiratory tract pathogens by gaseous contact. *J Antimicrob. Chemother*. 2001. 47(5) 565-573.

Inouye S., Abe S., Yamaguchi H., Asakura M. Comparative study of antibacterial and cytotoxic effects of selected essential gaseous and solution contacts. *J. Antimicrob Chemother*. 2003. (47) 565-573.

Isshiki K., Tokuoka K., Mori R., Chiba S. Preliminary examination of allyl isothiocyanate vapor for food preservation. *Biosci. Biotech. Biochem*. 1992. 56(9) 1476-1477.

Janiak C., Vieth J. K. MOFs, MILs and more: concepts, properties and applications for porous coordination networks (PCNs). *New J. Chem*. 2010. (34) 2366-2388.

Kara, H. H., Xiao, F., Sarkar, M., Jin, T., Sousa, M. M., Liu, C., Tomasula, P. M., & Liu L. Antibacterial poly(lactic acid) (PLA) films grafted with electrospun PLA/allyl isothiocyanate fibers for food packaging. *Journal of Applied Polymer Science*. 2015. 42475-42475.

Kawakishi S., Namiki M. Decomposition of allyl isothiocyanate in aqueous solution. *Agr. Bioi. Chem*., 1969. 33(3) 452-459.

Kawkishi S., Kaneko T. Interactions of proteins with allyl isothiocyanate. *J. Agric. Food Chem*. 1987. (35) 85-88.

Kesanli B., Cui Y., Smith, M. R., Bittner E. W., Bockrath B. C., Lin W. Highly interpenetrated metal-organic frameworks for hydrogen storage. *Angewandte Chemie International Edition*. 2005. (44) 72-75.

Keskin S., & Kizilel S. A review: biomedical applications of metal organic frameworks. *Industrial and Engineering Chemistry Research*. 2011, *50* (4), 1799–1812.

Kim Y. S., Ahn E. S., Shin D. H. Extension of shelf life by treatment with allyl isothiocyanate in combination with acetic acid on cooked rice. *Journal of food science*. 2002. 67(1) 274-279.

Kim W. T., Chung H., Shin I. S., Yam K. L., Chung D. Characterization of calcium alginate and chitosan-treated calcium alginate gel beads entrapping allyl isothiocyanate. *Carbohydrate Polymer*. 2008. (71) 566-573.

Ko J. A., Kim W. Y., Park H. J. Effects of microencapsulated allyl isothiocyanate (AITC) on the extension of the shelf life of Kimchi. *International Journal of Food Microbiology*. 2012. (153) 92-98.

Kojima M., Ogawa K. Studies on the effects of isothiocyanates and their analogous on microorganisms. I. Effect of isothiocyanates on the oxygen uptake of yeasts. *J. Ferment. Technol*. 1971. (49) 740-746.

Kuppler, R. J., Timmons, D. J., Fang, Q., Li, J., Makal, T. A., Young, M. D., Yuan, D., Zhao, D., Zhuang, W., & Zhou, H. Potential applications of metal-organic frameworks. *Coordination Chemistry Reviews*. 2009. (253) 3042-3066.

Küsgens, P., Rose, M., Senkovska, I., Fröde, H., Henschel, A., & Siegle, S. Characterization of metal-organic frameworks by water adsorption. *Microporous and Mesoporous Materials*. 2009. (120) 325-330.

Laird, K., & Philips, C. Vapor phase: a potential future use for essential oils as antmicrobials? *Letters in Applied Microbiology*. 2011. (54) 169-174.

Lan A., Li K., Wu H., Kong L., Nijem N., Olsen D. H., Emge T. J., Chabal Y. J., Langreth D. C., Hong M., Li J. RPM3: A multifunctional microporous MOF with recyclable framework and high H_2 binding energy. *Inorg. Chem*. 2009. (48) 7165-7173.

Lee J. Y., Pan L., Kelly S. P., Jagiello J., Emge T. J., Li J. Achieving high density of adsorbed hydrogen in microporous metal organic framework. Adv. Mater. 2005. (17) 2703-2706.

Lewis R. J. Sax's properties of industrial materials. 11th Edition. Wiley-interscience, Wiley & sons, Inc. Hoboken, NJ. 2004. p 119.

Li H., Eddaoudi M., O'Keeffe M., Yaghi O. Design and synthesis of an exceptionally stable and highly porous metal-organic framework. *Nature*. 1999. (402). 276-

Li Y., Yang R. T. Gas adsorption and storage in metal-organic framework MOF-177. Langmuir. 2007. 23(26) 12937-12944.

Li X., Jin Z., Wang J. Complexation of allyl isothiocyanate by α- and β-cyclodextrin and its controlled release characteristics. *Food Chemistry*. 2007. (103) 461-466.

Li W., Liu L., Jin T. Z. Antimicrobial activity of allyl isothiocyanate used to coat biodegradable composite films as affected by storage and handling conditions. *Journal of Food Protection*. 2012. 75(12) 2234-2237.

Lin C., Preston J. F., Wei C. Antibacterial mechanism of allyl isothiocyanate. *Journal of food protection*. 2000. 63(6) 727-734.

Lin S., Song Z., Che G., Ren A., Li P., Liu C. Adsorption behavior of metal-organic-frameworks for methylene blue from aqueous solution. *Microporous mesoporous Material*. 2014. (193) 27-34.

Lin K. A., & Hsieh Y. Copper-based metal organic framework (MOF), HKUST-1, as an efficient adsorbent to remove para-nitrophenol from water. *Journal of the Taiwan Institute of Chemical Engineering*. 2015. (50) 223-228.

Liu T., Yang T. Stability and antimicrobial activity of allyl isothiocyanate during long-term storage in an oil-in-water emulsion. *Journal of Food Science*. 2010. 75(5) C445-C451.

McKinlay A. C., Morris R. E., Hocajada P., Férey G., Gref R., Couvreur P., Serre C. BioMOFs: metal-organic frameworks for biological and medicinal applications. *Angew. Chem. Int. ed*. 2010. (49) 6260-6266.

Mari M., Leoni R. L., Cembali T. Antifungal vapor-phase activity of allyl-isothiocyanate against *Penicillium expansum* on pears. Plant Pathology. 2002. (51) 231-236.

Moellmer, J., Moeller, A., Dreisbach, F., Glaeser, R., & Staudt, R. (2011). High pressure adsorption of hydrogen, nitrogen, carbon dioxide and methane on the metal-organic framework HKUST-1. *Microporous and Mesoporous Materials, 138*, 140-148.

Mueller U., Schubert M., Teich F., Puetter H., Schierle-Arndt K., Pastre J. Metal-organic frameworks-prospective industrial applications. *J. Mater Chem*. 2006. (16) 626-636.

Nadarajah D., Han J. H., Holley R. A. Inactivation of *Escherichia coli* O157:H7 in packaged ground beef by allyl isothiocyanate. *International Journal of Food Microbiology*. 2005. (99) 269-279.

Neoh T. L., Yamamoto C., Ikefuji S., Furtuta T., Yoshii H. Heat stability of allyl isothiocyanate and phenyl isothiocyanate complexed with randomly methylated β-cyclodextrin. *Food Chemistry*. 2012. (131) 1123-1131.

Nielsen P. V., Rios R. Inhibition of fungal growth on bread by volatile components from spices and herbs, and the possible application in active packaging, with special emphasis on mustard essential oil. *International Journal of Food Microbiology*. 2000. (60) 219-229.

Ohta Y., Takatani K., Kawakishi S. Decomposition rate of allyl isothiocyanate in aqueous solutions. *Biosci. Biotech. Biochem*. 1995. (59) 102-103.

Otoni, C. G., Soares, N. F. F., Silva, W. A., Medeiros, E. A. A., & Baffa Junior, J. C. Use of allyl isothiocyanate-containing sachets to reduce *Aspergillus flavus* sporulation in peanuts. *Packaging Technology and Science*. 2014. (27) 549–558.

Otoni, C. G., Espitia P. J., Avena-Bustillos, R. J., McHugh T. H. Trends in antimicrobial food packaging systems: emitting sachets and absorbent pads. *Food Research International.* 2016. (83) 60-73.

Padukka I., Bhandari B., D'Arcy B. Evaluation of various extractions methods of encapsulated oil from β-cyclodextrin-Lemon oil complex powder. *Journal of food composition and analysis*. 2000. (13) 59-70.

Pan L., Olsen D. H., Ciemnolonski L. R., Heddy R. Li J. Separation and hydrocarbons with a microporous metal-organic frameworks. *Angew. Chem*. 2006. (118) 632-635.

Park S. Y., Barton M., Pendelton P. Mesoporous silica as a natural antimicrobial carrier. *Colloids and Surfaces*. 2011. (385) 256-261.

Park S. Y., Barton M., Pendelton P. Controlled release of allyl isothiocyanate for bacteria growth management. *Food Control*. 2012. (23) 478-484.

Passarinho A. T., Dias N. F., Camilloto G. P., Cruz R. S., Otoni C. G., Morales A. R., Soares N. F. Sliced bread preservation through oregano essential oil-containing sachet. *Journal of Food Processing Engineering*. 2014. (37) 53-62.

Pecháček R., Velíšek J., Hrabcová H. Decomposition products of allyl isothiocyanate in aqueous solutions. *J. Agric. Food Chem*. 1997. (45) 4584-4588.

Piercey M. J., Mazzanti G., Budge S. M., Delaquis P. J., Paulson A. T., Hansen L. T. Antimicrobial activity of cyclodextrin entrapped allyl isothiocyanate in a model system and packaged fresh-cut onions. *Food Microbiology*. 2012. (30) 213-218.

Pires, A. C. S., Soares, N. F. F., Andrade, N. J., Silva, L. H. M., Camilloto, G. P., & Bernardes, P. C. Increased preservation of sliced mozzarella cheese by antimicrobial sachet incorporated with allyl isothiocyanate. *Brazilian Journal of Microbiology.* 2009. (40) 1002–1008.

Plackett, D., Ghanbari-Siahkali, A., & Szente, L. Behavior of α- and β-cyclodextrin-encapsulated allyl isothiocyanate as slow-release additives in polylactic-co-polycaprolactone films. *Journal of Applied Polymer Science*. 2007. (105) 2850-2857.

Rosi, N. L., Kin, J., Eddaoudi, M., Chen, B., O'Keeffe, M., & Yaghi, O. M. Rod packing and metal-organic frameworks constructed from rod-shaped secondary building units. *Journal of American Chemical Society*. 2005. (127) 1504-1518.

Rowsell, J. L., & Yaghi, O. M. Effects of functionalization, catenation, and variation of the metal oxide and organic linking units on the low-pressure hydrogen adsorption properties of metal-organic frameworks. *Journal of American Chemical Society*. 2006. (128) 1304-1315.

Seo, H. -S., Bang, J., Kim, H., Beuchat, L. R., Cho, S. Y., & Ryu, J. H. Development of an antimicrobial sachet containing encapsulated allyl isothiocyanate to inactivate *Escherichia coli* O157:H7 on spinach leaves. *International Journal of Food Microbiology.* 2012. (159) 136–143.

Sekiyama Y., Mizukamin Y., Takada A., Oosono M. Effect of mustard extract vapor on fungi and spore-forming bacteria. Journal of Antibacterial and Antifungal agents. 1996. (24) 171-178.

Shin J., Harte B., Selke S. Active packaging of fresh chicken breast, with allyl isothiocyanate (AITC) in combination with modified atmosphere packaging (MAP) to control the gowth pathogens. *Journal of Food Science*. 2010. 75(2) M65-M71.

Siahaan E. A., Pendelton P., Woo H. Chun B. S. Brown seaweed (*Saccharina japonica*) as an edible natural delivery matrix for allyl isothiocyanate inhibiting food-borne bacteria. *Food Chemistry*. 2014. (152) 11-17.

Stofberg J., & Grundschober F. The consumption ratio and food predominance of flavoring materials. Perfumer flavorist. 1987. (12) 27-56.

Tony M., Jonchiere R., Pullumbi P., Coudert F., & Fuchs A. H. How can a hydrophobic MOF be water-unstable? Insight into the hydration mechanism of IRMOFs. *Chem. Phys. Chem*. 2012. (13) 3497-3503.

Trivedi N. A., Hotchandani S. C. A study of the antimicrobial activity of oil of Eucalyptus. *Indian J. Pharmacol.* 2004. (36) 93-94.

Tyagi A. K., Malik A. Antimicrobial action of essential oil vapors and nagative air ions against *Pseudomonas florescence*. *International Journal of Food Microbiology*. 2010. (143) 205-210.

Vegas-Lugo A.-C., Lim L. T. Controlled release of allyl isothiocyanate using soy protein and poly(lactic acid) electrospun fibers. *Food Research International*. 2009. (42) 933-940.

Vaughn J., Wu H., Efremovska B., Olsen D., Mattai J., Ortiz C., Puchalski A., Li J., Pan L. Encapsulated recyclable porous materials: an effective moisture-triggered fragrance release system. *Chem. Commun*. 2013. (49) 5724-5726.

Wang, H., Lashkari, E., Lim H., Zheng, C., Emge, T., Gong, Q., Yam, K., & Li, J. The moisture-triggered controlled release of a natural food preservative from a microporous metal–organic framework. *Chemical Communications*. 2016. (*52*) 2129-2132.

Ward S. M., Dealquis P. J., Holley R. A., Mazza G. Inhibition of spoilage and pathogenic bacteria on agar and pre-cooked roast beef by volatile horseradish distillates. *Food Research International*. 1995. 31(1) 19-26.

Winther M., Nielsen V. Active packaging of cheese with allyl isothiocyanate, an alternative to modified atmosphere packaging. *Journal of Food Protection*. 2006. 69(10) 2430-2435.

Wu T., Shin L., Luebbers M., Hu C., Chen Q., Ni Z., Masel R. I. Enhancing the stability of metal-organic frameworks in humid air by incorporating water repellent functional groups. *Chem. Commun*. 2010. (46) 6120-6122.

Wu H., Gong Q., Olsen D. H., Li J. Commensurate adsorption of hydrocarbons and alcohols in microporous metal organic frameworks. *Chemical Reviews*. (2012). (112) 836-868.

Xu W. W., Pramanik S., Zhang Z., Emge T. J., Li J. Micrporous metal organic framwork [*M*=Zn, Co; H2hfipbb=4,4-(hexafluoroisopropylidene)-bis(benzoic acid); ted-

triethylenediamine): synthesis, structure analysis, pore characterization, small gas adsorption and CO_2/N_2 separation properties. *Journal of Solid-State Chemistry*. 2013. (200) 1-6.

Yaghi O., & Li H. Hydrothermal synthesis of a metal organic framework containing large rectangular channels. *Journal of American Chemist Society*. 1995. (117) 10401.

Yaghi O., O' Keeffe M., Ockwig N. W., Chae H. K., Eddaoudi, M., Kim J. Reticular synthesis and the design of new materials. *Nature*. 2003. (423) 705-710.

Zaworotko M. J. There is plenty room in the middle: crystal clear opportunities abound for coordination polymers. *New Journal of Chemistry*. 2010. (34) 2355-2356.

Zhang J., Wu H., Emge T. J., Li J. A flexible MMOF exhibiting high selectivity for CO_2 over N_2, CH_4, and other small gases. *Chem. Commune*. 2010. (46) 9152-9154.